Current Challenges in Diagnosis and Assessment of the Response of Locally Advanced and Metastatic Renal Cell Carcinoma

Alberto Diaz de Leon, MD
Ali Pirasteh, MD
Daniel N. Costa, MD
Payal Kapur, MD
Hans Hammers, MD, PhD
James Brugarolas, MD, PhD
Ivan Pedrosa, MD, PhD

Abbreviations: AUA = American Urological Association, FDA = U.S. Food and Drug Administration, HIF = hypoxia-inducible factor, mTOR = mammalian target of rapamycin, RCC = renal cell carcinoma, RECIST = Response Evaluation Criteria in Solid Tumors, VHL = von Hippel-Lindau

RadioGraphics 2019; 39**:**998–1016

https://doi.org/10.1148/rg.2019180178

Content Codes: GU MR OI

From the Department of Radiology (A.D.d.L., A.P., D.N.C., I.P.), Advanced Imaging Research Center (D.N.C., I.P.), Department of Pathology (P.K.), Department of Urology (P.K.), Kidney Cancer Program–Simmons Comprehensive Cancer Center (P.K., H.H., J.B., I.P.), and Department of Internal Medicine (H.H., J.B.), UT Southwestern Medical Center, 5323 Harry Hines Blvd, Dallas, TX 75390. Presented as an education exhibit at the 2017 RSNA Annual Meeting. Received May 15, 2018; revision requested June 6 and received July 12; accepted July 26. For this journal-based SA-CME activity, the authors, editor, and reviewers have disclosed no relevant relationships. **Address correspondence to** I.P. (e-mail: *Ivan.Pedrosa@UTSouthwestern.edu*).

Supported by the National Institutes of Health (R01CA154475, P50CA196516).

SA-CME LEARNING OBJECTIVES

After completing this journal-based SA-CME activity, participants will be able to:

■ Discuss the common protocols recommended after nephrectomy for imaging surveillance of recurrent RCC and limitations associated with these surveillance strategies.

■ Describe tumor heterogeneity and the challenge it may present in assessment of treatment response.

■ Identify the potential limitations of size-based response criteria in assessment of treatment response to systemic therapy and list the common challenges radiologists may encounter with these agents.

See rsna.org/learning-center-rg.

Locally advanced and metastatic renal cell carcinoma (RCC) present a specific set of challenges to the radiologist. The detection of metastatic disease is confounded by the ability of RCC to metastasize to virtually any part of the human body long after surgical resection of the primary tumor. This includes sites not commonly included in routine surveillance, which come to light after the patient becomes symptomatic. In the assessment of treatment response, the phenomenon of tumor heterogeneity, where clone selection through systemic therapy drives the growth of potentially more aggressive phenotypes, can result in oligoprogression despite overall disease control. Finally, advances in therapy have resulted in the development of immuno-oncologic agents that may result in changes that are not adequately evaluated with conventional size-based response criteria and may even be misinterpreted as progression. This article reviews the common challenges a radiologist may encounter in the evaluation of patients with locally advanced and metastatic RCC.

Introduction

Renal cell carcinoma (RCC) is the most common primary renal malignancy, accounting for 90% of all renal malignancies. The most common subtype is clear cell RCC, followed by papillary and chromophobe subtypes. Each different histologic subtype is associated with distinct oncologic behavior and prognosis (1,2). Worldwide, kidney cancer is the 13th most common malignancy, and in the United States, the incidence of kidney cancer increased by 1.1% from 2004 to 2013 (3). Currently, the 5-year survival rate for kidney cancer is approximately 74%, which is an increase from 57% in 1987 (4).

Fortunately, the majority of patients (65%) with RCC have localized disease when they receive their diagnosis, while 16% of patients have RCC that has spread to regional lymph nodes, and another 16% have metastatic disease (4). The 5-year survival rate and risk of recurrent disease after resection are affected by various factors such as tumor grade, stage, and subtype of RCC.

TEACHING POINTS

- RCC has been reported to metastasize to virtually any part of the human body, with case reports showing metastases to the scalp; oral cavity; salivary, thyroid, and parathyroid glands; testicles; and penis. Infrequent sites of disease include the spleen, pleura, kidney, and ovaries. This may delay the detection of metastatic disease, because some sites such as the head and neck are not included in routine surveillance imaging for metastatic disease, and spread to these sites may be identified only after the patient becomes symptomatic.
- As with most malignancies, the time of greatest risk for recurrence of RCC is early after treatment, with the median time to relapse within 1–2 years after surgery. However, numerous case reports have documented recurrence more than 10 years after resection. To our knowledge, no formal recommendations exist for surveillance imaging beyond 5 years. One such site classically associated with delayed presentation of recurrent disease is the pancreas.
- RCC is characterized by tumor heterogeneity, a phenomenon in which different clones of cells with specific genomic alterations coexist in the primary tumor and possibly even metastases. Clone selection through systemic therapy drives the growth and survival of certain subclones and possibly more aggressive phenotypes.
- Compared with traditional cytotoxic therapies, molecular-targeted agents may result in changes in the tumor microenvironment such that a response may not be solely reflected in a change in size.
- Immune modulators have resulted in a further challenge, because their mechanism of action, through immune and T-cell activation, can result in unusual patterns of response. Infiltration of tumor deposits by immune cells can result in a transient increase in lesion size (and visualization of new lesions) compared with those at initial imaging, followed by tumor regression, which is a phenomenon known as pseudoprogression.

The radiologist plays an essential role in the care of patients with RCC. However, metastatic RCC presents challenges to the radiologist, including the ability of RCC to invade locally and/or metastasize to a number of unusual sites many years after resection of the primary tumor. Although the advent of targeted and immune therapies, stereotactic radiation therapy, and various percutaneous ablation techniques has revolutionized the treatment of patients with metastatic RCC, these therapies have presented new issues that may confound the interpretation of disease response. This article reviews the common challenges a radiologist may encounter in patients with metastatic RCC.

Background

RCC Subtypes and Their Imaging Characteristics

There are multiple subtypes of RCC that are differentiated by various histopathologic features such as cytoplasmic and architectural features, anatomic location within the kidney, and molecular alterations. The most common subtype of RCC is clear cell RCC, which accounts for approximately 70% of cases (1). At histopathologic examination, clear cell RCC is differentiated from other subtypes by nests of cells with clear, lipid-containing cytoplasm characteristically surrounded by an extensive capillary network (5). Clear cell RCC is associated with a worse prognosis than are papillary RCC and chromophobe RCC (6,7).

At CT and MRI, hypervascularity that occurs during the corticomedullary phase, with peak enhancement of as much as or greater than that of the renal cortex, is the characteristic feature of clear cell RCC (8,9). At MRI, clear cell RCC tends to appear hyperintense on T2-weighted images; the presence of lipid within the cytoplasm of clear cell RCC is reflected on out-of-phase T1-weighted images as a relative decrease in signal intensity compared with that on in-phase images. At diffusion-weighted MRI, clear cell RCC can have various appearances with a range of apparent diffusion coefficients reported, although high-grade clear cell RCC has been reported to have significantly lower apparent diffusion coefficients compared with those of low-grade clear cell RCC (10,11).

The second most common subtype of RCC is papillary RCC, which accounts for 15%–20% of cases (1). Compared with clear cell RCC, papillary RCC is more often multifocal and bilateral. Papillary RCC is divided into two subtypes. Type 1 papillary RCC tumors have cells with scant pale cytoplasm arranged as a single layer along a papillary core (12). Type 2 papillary RCCs are characterized by cells with pseudostratified nuclei and voluminous eosinophilic cytoplasm (12). Compared with the type 1 subtype, type 2 papillary RCC is associated with a worse prognosis, in addition to a higher tumor stage and grade. Nevertheless, a subset of tumors have mixed histologic features, and recent studies suggest that type 2 tumors may be composed of individual subtypes with specific molecular alterations rather than a single subtype (13).

At imaging, papillary RCC is characteristically hypovascular compared with clear cell RCC, enhancing to a lesser degree compared with the renal cortex (9). Intralesional hemorrhage is common and can result in signal hyperintensity and hypointensity on T1- and T2-weighted images, respectively. Papillary RCC also can manifest as a complex cystic mass containing hemorrhagic contents and mural hypoenhancing nodules. Features may overlap between type 1 and type 2 subtypes of papillary RCC, although type 2 papillary RCCs tend to be larger. Similarly, papillary RCC type 2 manifests more often with an infiltrative pattern and renal vein invasion, both of which are features associated with worse prognosis (14,15).

Several new subtypes of RCC recently were recognized in the 2016 World Health Organization classification (13), including hereditary leiomyomatosis RCC, succinate dehydrogenase–deficient RCC, tubulocystic RCC, acquired cystic disease–associated RCC, and clear cell papillary RCC. Hereditary leiomyomatosis RCC is a rare autosomal-dominant condition caused by a germline loss of function mutation in the fumarate hydratase gene and is characterized by the presence of cutaneous and uterine leiomyomas and RCC. The histologic and imaging appearance of hereditary leiomyomatosis RCC is in keeping with the type 2 papillary RCC subtype and is associated with a poor prognosis (16). Patients with germline mutations in succinate dehydrogenase–deficient genes are predisposed to developing succinate dehydrogenase–deficient RCC, in addition to paragangliomas, and the tumors tend to develop in young adults (17). However, to our knowledge, the imaging characteristics of succinate dehydrogenase–deficient RCC have not yet been well described.

Tubulocystic RCC is a rare tumor and is reported to occur more commonly in male patients (18). At imaging, tubulocystic RCC has been reported to manifest as a complex cystic mass and may show features of a Bosniak IIF, III, or IV cystic lesion (19,20). Patients with end-stage kidney disease and three or more cysts per kidney are defined as having acquired cystic kidney disease (21). Previously, papillary RCC was reported to be the most common subtype of RCC in patients with acquired cystic kidney disease.

Acquired cystic kidney disease–associated RCC is a distinct subtype with specific histologic features, including cribriform architecture and calcium oxalate crystal deposition, and is now reported to be the most common subtype of RCC in patients with acquired cystic kidney disease (22,23).

Clear cell papillary RCC is characterized at histopathologic examination as containing papillary and clear cell components and is reported to occur more commonly in patients with chronic kidney disease as well (24). This subtype is thought to have a low potential for malignancy and a favorable prognosis (25,26). A broad spectrum of imaging features has been described, including a predominantly complex cystic appearance and a predominantly solid heterogeneous or homogeneous mass, with hypo- and hyperenhancing solid areas, which make it challenging to differentiate clear cell papillary RCC from papillary RCC and clear cell RCC at imaging (27,28).

Tumor Biology of Clear Cell RCC

The discovery of the von Hippel-Lindau (*VHL*) gene and its role in the development of clear cell RCC was pivotal in advancing the understanding of the biology of this tumor and developing new therapeutic agents. The protein encoded by the *VHL* gene, pVHL, is a critical component in the hypoxia pathway, because it regulates the hypoxia-inducible factor (HIF) (29). When oxygen is available, pVHL designates HIF for degradation. In a patient with hypoxia, HIF is not labeled, and this results in the expression of multiple angiogenic factors such as vascular endothelial growth factor, platelet-derived growth factor, and transforming growth factor. Therefore, mutations inactivating the *VHL* gene result in deregulated expression of HIF-responsive genes (with hypoxia response elements in their promoters), and ultimately, the formation of new blood vessels (ie, neoangiogenesis), which facilitates tumor growth.

The mammalian target of rapamycin (mTOR) protein also has a role in the regulation of HIF, such that mTOR promotes HIF activity (30). These insights have driven the development of targeted therapies. Vascular endothelial growth factor and platelet-derived growth factor induce angiogenesis through acting on their cognate receptor tyrosine kinases. The vascular endothelial growth factor pathway is inhibited by several drugs approved by the U.S. Food and Drug Administration (FDA) for the treatment of advanced RCC including bevacizumab, a neutralizing vascular endothelial growth factor antibody, and tyrosine kinase inhibitors such as sorafenib, sunitinib, pazopanib, axitinib, cabozantinib, and lenvatinib. Everolimus and temsirolimus are also FDA-approved drugs for the treatment of advanced RCC that inhibit mTOR complex 1. HIF-2 inhibitors have been developed in recent years and are currently under investigation (31–33).

Like many malignancies, RCC exploits immune checkpoint pathways to evade targeting by the immune system. Normally, the immune system is able to identify and eliminate abnormal cancerous cells by recognizing neoantigens expressed on the tumor cells. Cytotoxic T-lymphocytes require signals to become activated and are regulated by checkpoint pathways. Cytotoxic T-lymphocyte antigen 4 and programmed cell death-1 and its ligand are examples of molecules implicated in T-cell regulation that are the targets of FDA-approved inhibitors such as nivolumab and ipilimumab, which have demonstrated activity in patients with RCC.

Imaging Assessment and Challenges in Detection

Surveillance Strategies

The primary treatment of localized RCC is surgical resection through partial or radical nephrec-

tomy, and imaging after therapy is necessary to identify recurrent disease. To our knowledge, a universally accepted imaging surveillance strategy has not yet been established, but current guidelines suggest imaging on the basis of the risk-adapted protocol and patterns of recurrence. The rate and timing of recurrence after therapy and local or distant metastatic recurrence vary and are dependent on several factors such as tumor grade, stage, and histologic features (eg, the presence of sarcomatoid component) (34–36).

Certain subtypes such as clear cell RCC are more likely to metastasize; one recent study of 41 836 patients with metastatic RCC found that 79% were related to clear cell RCC (37). Recurrence most often occurs within the first 3 years after surgery. The reported recurrence rate after partial or radical nephrectomy may be as low as 15%–20% for patients with low-risk disease (pT1, N0 or NX) and has been reported to reach nearly 70% for patients with moderate- to high-risk disease (pT2–4, N0 or N1) (38–41). The most common sites of recurrence include the lung, bone, lymph nodes, adrenal gland, liver, and, less frequently, the brain (41–43).

Most guidelines suggest imaging of the chest and abdomen, taking into account the common sites of recurrence. In patients with low-risk disease after partial nephrectomy (eg, localized T1 disease), the American Urological Association (AUA) and the National Comprehensive Cancer Network (NCCN) guidelines advocate baseline imaging of the abdomen with contrast material–enhanced CT or MRI within 3–12 months after surgery and chest radiography 12 months after surgery. CT is more likely to allow identification of recurrences in the chest, although given the cost, radiation exposure, false-positive results (eg, lung granulomas), and the low likelihood of recurrence in patients at low risk, chest radiography is the preferred modality. If chest radiography shows an abnormality suspicious for metastatic disease (eg, lymphadenopathy, a nodule, or a mass), CT should be performed for further evaluation. A more aggressive surveillance approach usually is followed for those with moderate- and high-risk disease (ie, T2 and T3 disease) (39). AUA and NCCN guidelines recommend baseline imaging at 3 months with contrast-enhanced CT of the chest and contrast-enhanced CT or MRI of the abdomen followed by repeat imaging at least at 6-month intervals for the first 3 years and yearly until 5 years.

The American College of Radiology provides similar recommendations in asymptomatic patients with no known metastases after primary treatment of RCC. Chest radiography usually is considered appropriate, unless the patient is at high risk for metastatic disease; otherwise, CT of the chest with intravenous contrast material is recommended. For imaging of the abdomen and pelvis, contrast-enhanced CT and MRI are considered equally appropriate.

Ideally, all imaging should be performed with intravenous contrast material. A large percentage of patients meet criteria for chronic kidney disease after partial and radical nephrectomy. In patients at risk for contrast material–induced nephropathy, including those older than 60 years or with a history of renal disease (eg, renal cancer, a single kidney, renal surgery, dialysis, renal transplant, hypertension requiring medical therapy, or diabetes), assessment of renal function before the intravascular administration of iodinated contrast medium is suggested, given the potential risk of contrast material–induced nephropathy (39). Although there is no specific threshold at which iodinated contrast material should not be administered, an estimated glomerular filtration rate of 30 mL per minute per 1.73 m^2 has been suggested (44). Nevertheless, the use of contrast material is essential for detection of metastatic disease in the majority of solid organs, particularly with CT.

In addition, with CT, dual-phase imaging during the arterial and portal venous phases is recommended in patients with RCC, because metastases to the liver and pancreas may be visible in only the arterial phase (45). In one study (46), 33% of liver metastases from RCC were detected in only the arterial phase. To our knowledge, studies in which the sensitivity of nonenhanced CT for the detection of metastatic disease were evaluated are lacking, specifically in patients with RCC. One study (47) in patients with gastrointestinal malignancies reported per-patient and per-lesion sensitivity for new hepatic metastases at nonenhanced CT of 56.1%–66.7% and 52.6%–56.8%, respectively.

Intravenous administration of gadolinium-based contrast agents at the standard dose is not considered nephrotoxic. The risk of nephrogenic systemic fibrosis is very low or possibly nonexistent in patients who receive standard or lower than standard doses of group II gadolinium-based contrast agents. Accordingly, the current American College of Radiology guidelines indicate that renal function assessment with a questionnaire or laboratory testing before administration of a standard dose of a group II gadolinium-based contrast agents is optional (48). Patients who receive a group I or group III gadolinium-based contrast agent should be screened for renal impairment. In patients with a contraindication to iodinated contrast material (ie, allergy or renal impairment), nonenhanced CT of the chest and MRI of the abdomen and pelvis can be performed.

The role of PET in patients with RCC is less obvious. PET/CT is not used routinely in the

Figure 1. Thyroid metastasis from clear cell RCC in a 53-year-old man. **(a)** Coronal CT image of the chest with intravenous contrast material shows a heterogeneous nodule in the left lobe of the thyroid (yellow arrow). Note the subtle residual cortical irregularity in the right fifth rib (white arrow), which is a sequela of a metastasis that had been treated previously with stereotactic radiation therapy. **(b)** Coronal CT image of the chest from an examination performed 2 years later shows interval enlargement of the left thyroid lesion (yellow arrow). Again note the subtle cortical irregularity in the right fifth rib (white arrow). **(c)** Thyroid US image from an examination performed soon after the CT examination in **b** shows a predominantly solid nodule with scattered cystic components in the left thyroid lobe (arrows). Fine-needle-aspiration biopsy allowed confirmation of metastatic RCC.

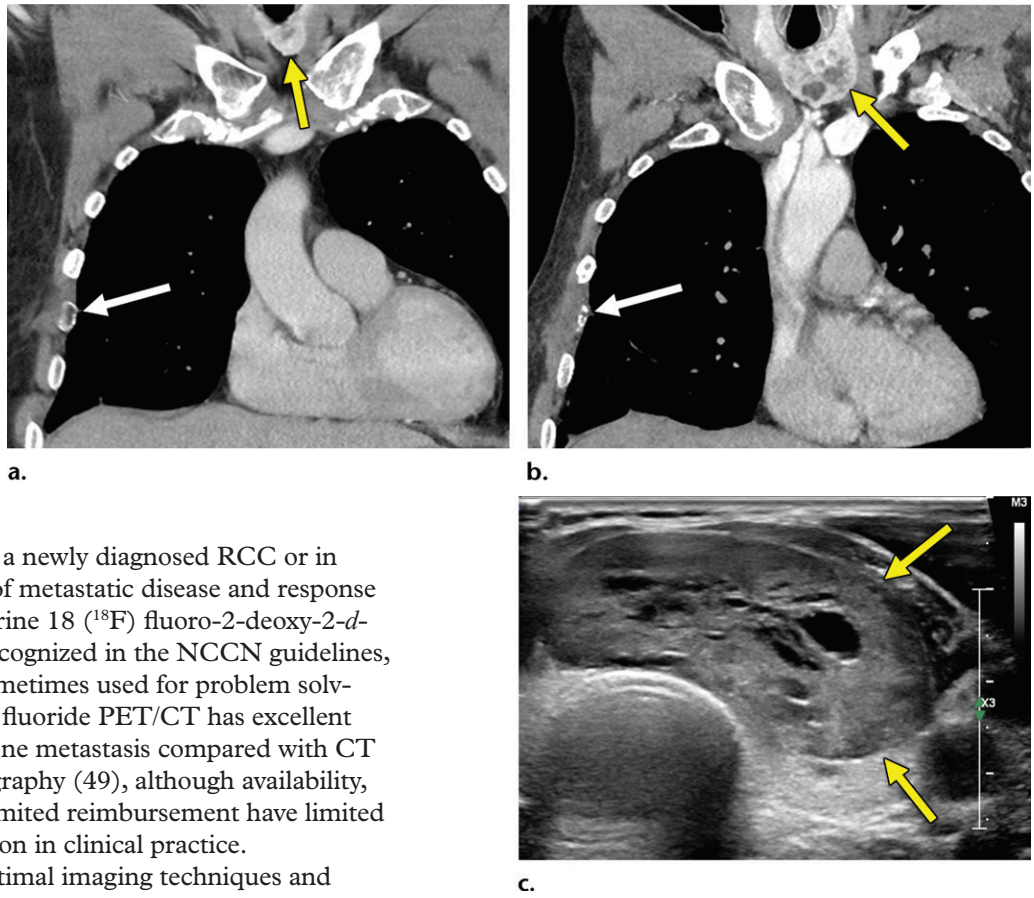

initial staging of a newly diagnosed RCC or in the assessment of metastatic disease and response to therapy. Fluorine 18 (^{18}F) fluoro-2-deoxy-2-*d*-glucose is not recognized in the NCCN guidelines, although it is sometimes used for problem solving. ^{18}F–sodium fluoride PET/CT has excellent sensitivity for bone metastasis compared with CT and bone scintigraphy (49), although availability, high cost, and limited reimbursement have limited its implementation in clinical practice.

Even with optimal imaging techniques and strategies, detecting recurrent and metastatic disease may be confounded by various factors including the propensity to metastasize to virtually any part of the human body, atypical patterns of manifestation, and limitations in technique. Because patients with metastatic disease live longer with new therapies, these tumors have the opportunity to metastasize to more locations, some of which may not be the most common targets for metastatic RCC.

Unusual Locations

RCC has been reported to metastasize to virtually any part of the human body, with case reports showing metastases to the scalp; oral cavity; salivary, thyroid, and parathyroid glands; testicles; and penis (50–52). Infrequent sites of disease include the spleen, pleura, kidney, and ovaries (53). This may delay the detection of metastatic disease, because some sites such as the head and neck are not included in routine surveillance imaging for metastatic disease, and spread to these sites may be identified only after the patient becomes symptomatic. In addition, one case series (49) of 36 patients with thyroid metastases showed an absence of clinical evidence for thyroid dysfunction (ie, hyper- or hypothyroidism), which may further confound initial detection (Fig 1). Nevertheless, even in sites that are imaged routinely as part of surveillance, identification of metastatic disease against normal anatomic structures may be difficult.

An RCC metastasis to the gastrointestinal tract and peritoneum is an uncommon phenomenon. Nevertheless, identification of gastrointestinal metastases is crucial, because they can result in various complications including gastrointestinal bleeding, obstruction, and biliary and pancreatic ductal dilatation in the uncommon case of duodenal metastases. In one study (43), small and large intestine metastases were identified in 1.3% and 1.1% of patients with metastatic RCC, respectively; peritoneal involvement was found in 7% of patients.

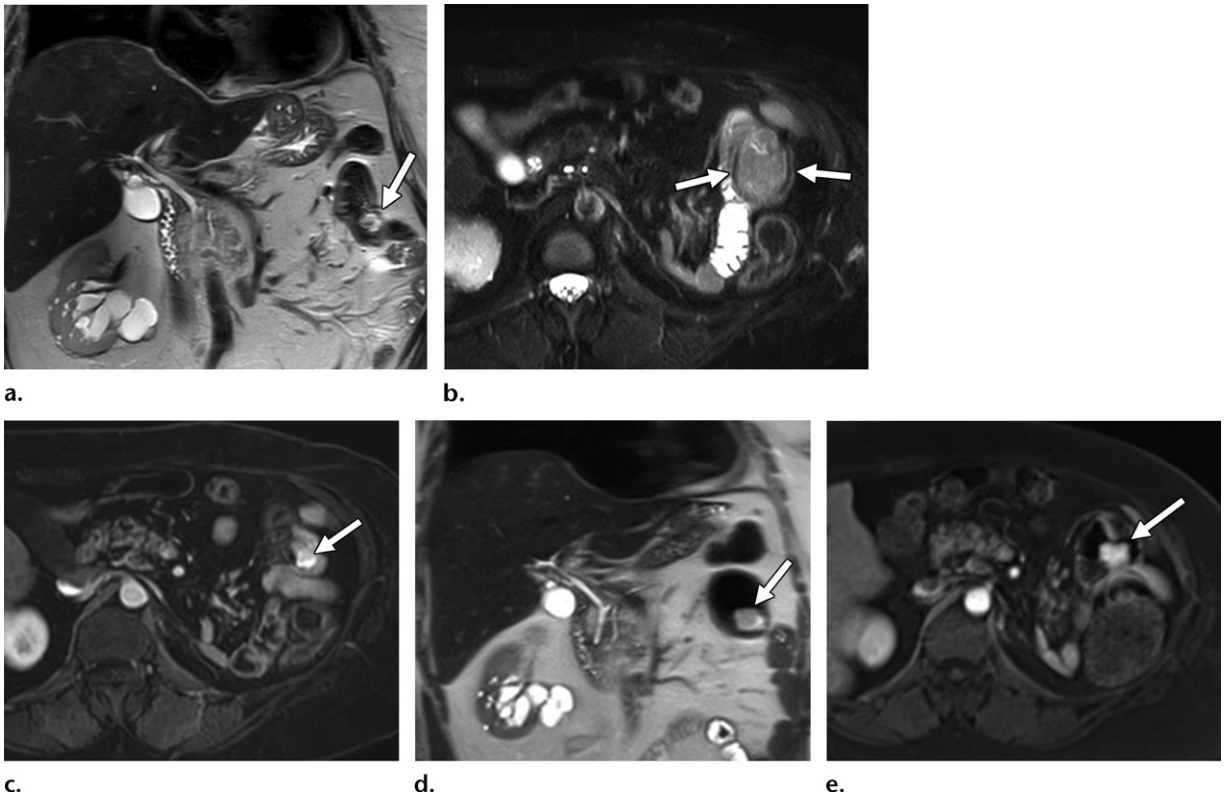

Figure 2. Clear cell RCC metastasis to the small bowel in a 57-year-old man. **(a–c)** Coronal T2-weighted **(a)**, axial fat-saturated T2-weighted **(b)**, and axial three-dimensional contrast-enhanced T1-weighted **(c)** MR images through the upper abdomen show a subtle intraluminal lesion in a segment of the jejunum (arrow in **a** and **c**). Note the hypervascular nature of the lesion exhibiting intense enhancement during the arterial phase (arrow in **c**), which is typical of clear cell RCC. During the MRI examination, the segment of the bowel with the lesion was intermittently undergoing intussusception (arrows in **b**), which obscured the abnormality. **(d, e)** Coronal T2-weighted **(d)** and axial contrast-enhanced arterial phase **(e)** MR images acquired 3 months later show that the abnormality has increased in size and is more readily visible (arrow).

Gastrointestinal metastases are reported to occur most commonly in the ileum and duodenum (43,54) and may manifest as avidly enhancing intraluminal polypoid lesions, exophytic submucosal lesions, or focal wall thickening. In addition, reports have described patients who presented with single or multiple intussusceptions secondary to intestinal metastases (55,56) (Fig 2). Peritoneal metastases can manifest as discrete avidly enhancing nodules, although widespread omental infiltration also has been described (57). Some RCC subtypes may have a predisposition for this pattern of spread. Peritoneal metastases are reported to be common with papillary RCC (58). In our experience, patients with hereditary leiomyomatosis and RCC also may have a higher predisposition for metastases to the omentum or peritoneum (Fig 3).

The detection of gastrointestinal tract metastases may be challenging at routine imaging of the abdomen and pelvis, because a large volume of enteric contrast material to distend the bowel lumen is not administered regularly unless there is a preexisting indication for small bowel assessment, where an appropriate enterographic technique may be implemented. In addition, positive oral contrast material, which could obscure avidly enhancing intraluminal lesions or peritoneal metastases near the bowel, may be administered during routine imaging, such as CT of the abdomen and pelvis. Similarly, at MRI, unless the small bowel is prepared with an adequate volume of oral contrast material, susceptibility and motion artifacts could obscure both gastrointestinal tract and peritoneal metastases. The use of positive oral contrast material increases the detection of mesenteric and peritoneal nodules, although hyperenhancing bowel contents may obscure enhancing bowel metastases (Fig 4).

In comparison, the use of negative oral contrast material increases the detection of enhancing bowel lesions, although peritoneal lesions may go undetected, because omental and mesenteric masses may be mistaken for nonenhancing bowel tissue. Currently, to our knowledge, there are no formal recommendations regarding the use of oral contrast material in the oncologic setting, and at our institution, we routinely use positive oral contrast material at CT performed for oncologic follow-up. The intense enhancement of clear cell RCC metastases also may challenge their

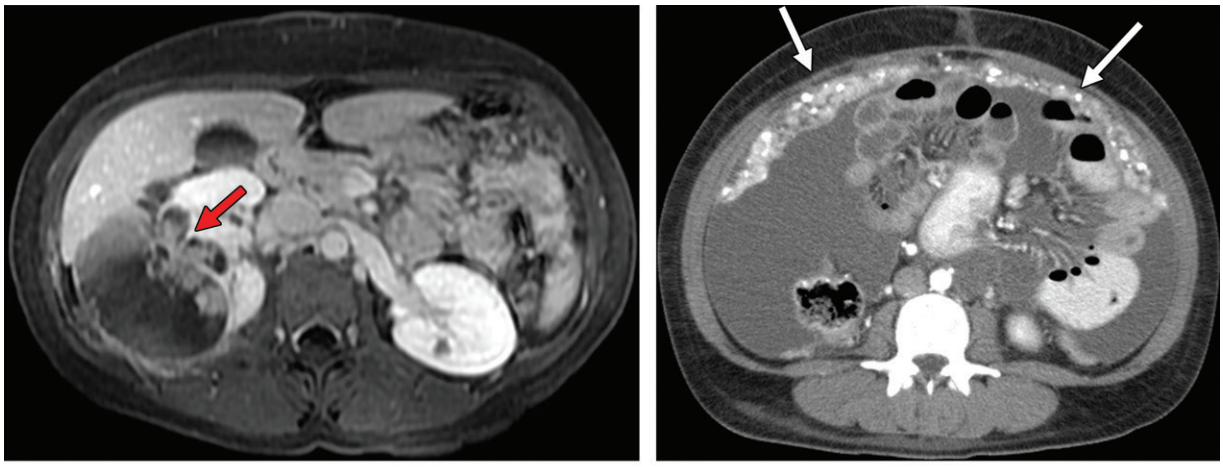

a. b.

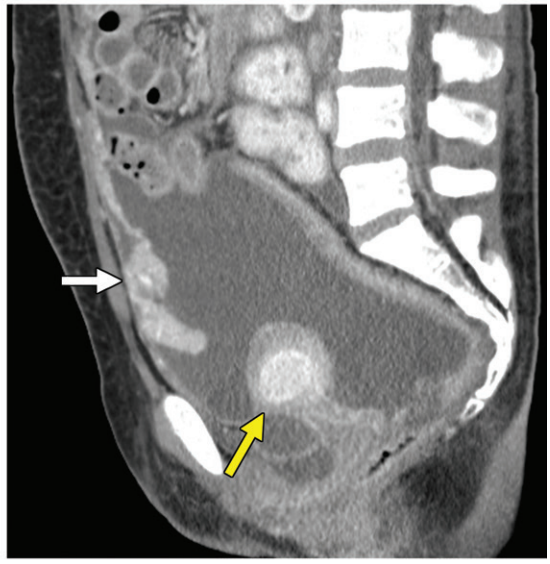

c.

Figure 3. Hereditary leiomyomatosis and RCC syndrome in a 30-year-old woman. **(a)** Axial contrast-enhanced T1-weighted MR image shows a right partially cystic renal tumor. Note the obvious infiltration of the renal parenchyma by the tumor (arrow). After nephrectomy, histopathologic evaluation and molecular assessment of the tumor disclosed fumarate hydratase–deficient RCC. **(b, c)** Axial **(b)** and sagittal **(c)** contrast-enhanced CT images acquired 1 year after nephrectomy show diffuse omental carcinomatosis (white arrows in **b** and **c**). An enhancing mass consistent with a leiomyoma is noted in the uterus (yellow arrow in **c**).

recognition compared with adjacent enhancing vascular structures.

Late Manifestations

As with most malignancies, the time of greatest risk for recurrence of RCC is early after treatment, with the median time to relapse within 1–2 years after surgery (40,41,59). However, numerous case reports (60–62) have documented recurrence more than 10 years after resection. To our knowledge, no formal recommendations exist for surveillance imaging beyond 5 years. One such site classically associated with delayed manifestation of recurrent disease is the pancreas. Overall, the pancreas is an uncommon site for metastatic disease, with a reported incidence of 1.3%–11%. Clear cell RCC is one of the more common primary tumors to metastasize to the pancreas (63). Patients with RCC and pancreatic metastasis tend to have more indolent disease than do other patients with metastatic RCC (64). Several patterns of manifestation have been described at imaging, including a solitary and well-defined metastasis and multifocal or diffuse infiltration of the gland with no predilection for a particular part of the gland (63,65).

At contrast-enhanced CT, pancreatic metastatic lesions are most often hypervascular and demonstrate avid early arterial phase enhancement followed by rapid washout in subsequent phases (45,66) (Fig 5). While metastases most often remain hyperattenuating in the portal venous phase relative to the background parenchyma, the difference in attenuation between the pancreas and metastasis is greatest during the arterial phase, with up to 9% of metastases seen only on arterial phase images (45).

At MRI, pancreatic metastases demonstrate similar findings to those of contrast-enhanced CT, although the inherent tissue contrast of MRI provides additional sequences to assist in lesion identification. The pancreatic parenchyma normally appears as uniform hyperintensity on nonenhanced T1-weighted MR images and allows the identification of pancreatic metastases, which appear as hypointensity relative to the surrounding parenchyma. It is important to scrutinize the pancreas carefully at nonenhanced T1-weighted fat-saturated MRI, because many pancreatic metastases become isointense (ie, imperceptible) when compared with the avidly enhancing pancreatic parenchyma after administration of gadolinium-based contrast material, even during the arterial phase. At T2-weighted MRI with or without fat saturation, metastases may appear hyper- or

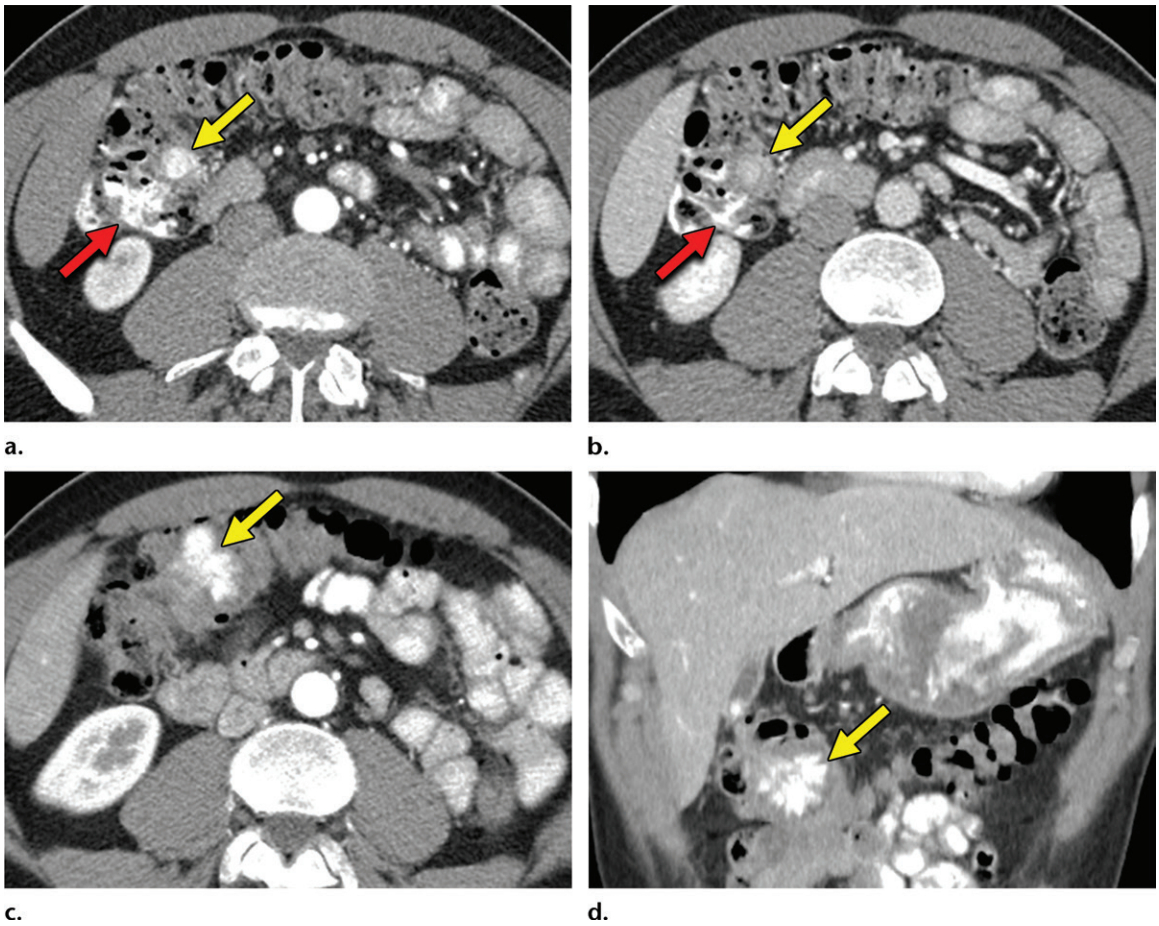

Figure 4. Metastatic clear cell RCC to the large bowel in a 54-year-old man. **(a, b)** Axial contrast-enhanced arterial phase **(a)** and portal venous phase **(b)** CT images of the upper abdomen show a subtle intraluminal lesion in the proximal transverse colon that appears nearly isointense (yellow arrow in **a**) compared with the oral contrast material (red arrow in **a**) in the adjacent colon on the arterial phase image. The lesion becomes hypointense (yellow arrow in **b**) relative to the oral contrast material in the adjacent colon (red arrow in **b**) during the portal phase acquisition. This lesion went undetected on several subsequent follow-up studies. **(c, d)** Axial **(c)** and coronal **(d)** CT images of the upper abdomen acquired 1.5 years later show that the intraluminal lesion has increased in size (yellow arrow) and resulted in a short-segment colocolic intussusception. Subsequent hemicolectomy allowed confirmation of metastatic clear cell RCC.

hypointense relative to the parenchyma, and at diffusion-weighted MRI, pancreatic metastases are more often hyperintense (67,68).

Pancreatic metastases can be differentiated from primary pancreatic adenocarcinoma. While pancreatic metastases can result in ductal dilatation, in our experience, it is less pronounced than in primary pancreatic adenocarcinoma, even in the presence of large metastatic lesions. Furthermore, pancreatic adenocarcinoma characteristically enhances less than the surrounding pancreatic parenchyma in the arterial phase and encases peripancreatic arteries and veins, which are uncommon features with pancreatic metastases (69,70). The imaging appearance of pancreatic metastases may overlap with that of neuroendocrine tumors at CT and MRI, because both are hypervascular and show variable signal intensity at T2-weighted MRI. However, pancreatic metastases are multiple more frequently than are neuroendocrine tumors (67). In addition, a recent study (71) suggested that pancreatic metastases may show a greater relative percentage of washout between the arterial and portal venous phases at CT than that of neuroendocrine tumors.

Adrenal Metastases

Depending on the pathway of extension of the tumor to the adrenal gland, the patient's cancer is staged differently on the basis of the tumor, lymph node, metastasis (TNM) staging system. RCC can affect the adrenal gland because of direct invasion of the ipsilateral gland (T4 disease) or because of hematogenous spread to either gland (metastatic disease). The latter results in separate adrenal nodules, which represent a diagnostic dilemma, particularly in patients with clear cell RCC and no prior imaging available for comparison. Clear cell RCC metastases can have overlapping imaging features with lipid-poor adenomas at adrenal washout CT (72). Similarly, both clear cell RCC metastasis and lipid-rich adenomas can exhibit lipid content

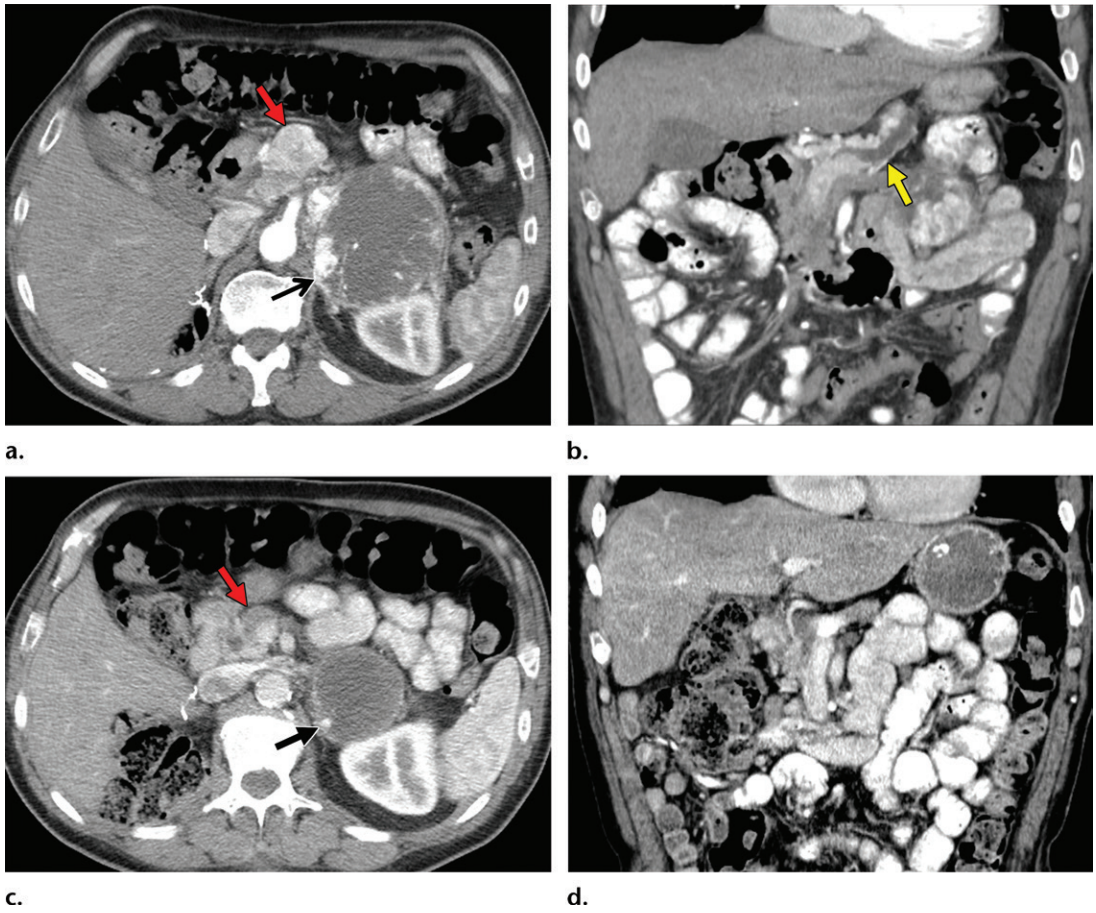

Figure 5. Metastatic RCC involving the pancreas and left adrenal gland in a 65-year-old man. **(a, b)** Axial **(a)** and coronal **(b)** contrast-enhanced CT images acquired during the arterial phase show an avidly enhancing mass in the pancreatic neck (red arrow in **a**) resulting in upstream dilatation of the pancreatic duct (arrow in **b**). A large left adrenal metastasis (black arrow in **a**) is present. The patient was subsequently administered ipilimumab and nivolumab. **(c, d)** Axial **(c)** and coronal **(d)** contrast-enhanced CT images from an examination performed 3 months after the initiation of therapy show a dramatic decrease in the size and enhancement of the pancreatic (red arrow in **c**) and adrenal (black arrow in **c**) metastases. Note the associated resolution of pancreatic ductal dilatation.

at chemical shift MRI. A recent study (73) suggested that hyperintensity and heterogeneity at T2-weighted MRI are more common in patients with adrenal metastasis than in those with adenomas.

Osseous Metastases

Osseous metastases deserve special mention, because unlike the gastrointestinal tract and pancreas, bone is a more common site for metastatic disease, and bone metastases are found in approximately 22%–30% of patients with metastatic RCC (43,74). Nevertheless, to our knowledge, the ideal method for the detection of osseous metastases in metastatic RCC has not been established.

Bone metastases from RCC are most often osteolytic and more commonly affect the axial skeleton. At CT, metastases manifest as a site of osseous lytic destruction and may show an associated enhancing soft-tissue mass. Osseous metastases can be distinguished from normal marrow signal intensity on nonenhanced T1-weighted and fat-saturated T2-weighted MR images, with lesions appearing hypointense and hyperintense, respectively, relative to fatty marrow. At diffusion-weighted MRI, metastases are most often hyperintense relative to marrow as well. On T2-weighted MR images, a rim of signal hyperintensity, which is postulated to be the result of destruction of trabeculae leading to a fluid-filled gap, has been described as specific for osseous metastases (75).

Early diagnosis is essential to guide therapy and help prevent skeletally related events such as pathologic fractures, spinal cord compression, and bone pain. While the axial skeleton is more often affected by metastatic disease, RCC metastases can occur in the appendicular skeleton as well. Therefore, the ideal method to detect osseous metastatic disease is screening of the entire skeleton.

A skeletal radiographic survey may be performed to identify a lytic metastasis that is at risk for pathologic fracture. To our knowledge, the sensitivity of a skeletal survey in patients with RCC has not been studied well. Bone scintigraphy with technetium 99m (^{99m}Tc) methylene diphosphonate

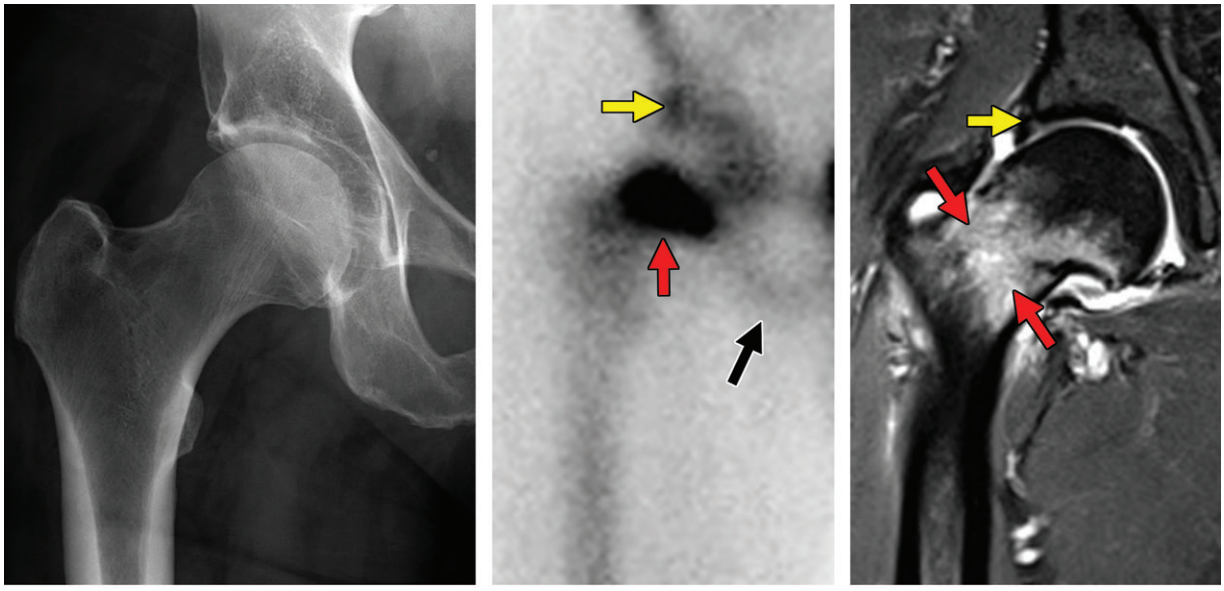

a. c. d.

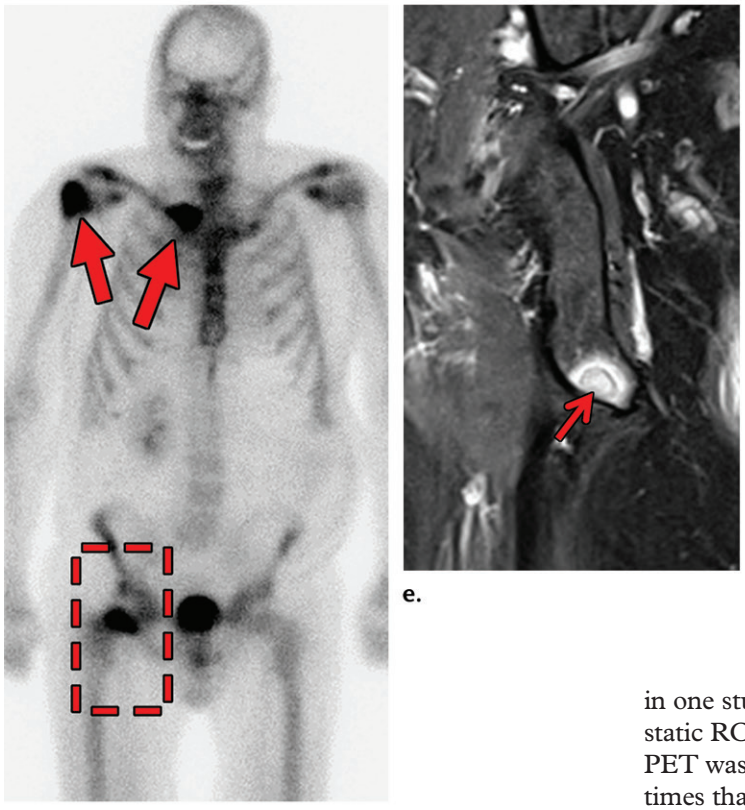

b. e.

Figure 6. Metastatic RCC and hip pain in a 63-year-old man. **(a)** Radiograph of the right hip shows no abnormalities. **(b)** ^{99m}Tc methylene diphosphonate bone scintigram shows lesions in the right humerus and the clavicle (arrows) and the right hip (dashed square). **(c)** Detail image of the right hip corresponding to the dashed square in **b** shows abnormal uptake in the right femoral head (red arrow) and a small area of increased uptake in the acetabulum (yellow arrow). **(d, e)** Coronal fat-saturated T2-weighted fast spin-echo MR images at the level of the femoral head **(d)** and the ischial tuberosity **(e)** show marrow edema in the femoral neck (red arrows in **d**) corresponding to the abnormality on the bone scan due to an insufficiency fracture. Mild degenerative changes are noted in the right acetabulum (yellow arrow in **d**), corresponding to the focus of uptake in the right acetabulum in **c**, but there is no evidence of metastasis. A metastasis in the right ischium (red arrow in **e**) is clearly shown on the MR images but not detected on the bone scintigram (black arrow in **c**).

provides a survey of the entire skeleton at a relatively low cost and is a standard initial method for screening the skeleton for metastatic disease. However, RCC metastases are most often lytic, with a limited osteoblastic response, resulting in poor uptake at bone scintigraphy. The reported sensitivity of scintigraphy for bone metastases from RCC is 10%–60% (76). ^{18}F-labeled sodium fluoride PET/CT has sensitivity of 98.7%–100% and specificity of 94.4% for the detection of metastatic disease; in one study (77) evaluating patients with metastatic RCC, the sensitivity of ^{18}F sodium fluoride PET was found to be twice that of CT and three times that of bone scintigraphy. However, despite excellent results, its lack of wide availability, high cost, and limited reimbursement have challenged the broad implementation of ^{18}F sodium fluoride PET/CT in clinical practice.

MRI provides numerous advantages including excellent contrast and spatial resolution, which allow for exquisite evaluation of both the cortical bone and bone marrow; the nonnephrotoxic nature of gadolinium-based contrast agents; and the lack of ionizing radiation. These attributes provide the opportunity for better characterization of metastatic and nonmetastatic lesions compared with that of bone scintigraphy (Fig 6). However,

the limited anatomic coverage and total examination time preclude the wide use of MRI for screening of the entire skeleton. Relatively recent improvements in MRI techniques have provided the opportunity to screen virtually the entire skeleton for metastatic disease. Several reports (78–80) have described the utility of whole-body MRI in patients with several types of malignancies. Similarly, whole-body MRI has demonstrated superior sensitivity to that of ^{99m}Tc methylene diphosphonate bone scintigraphy and CT for detection of RCC osseous metastases (81,82).

Challenges in Response Assessment

The assessment of response to therapy in patients with metastatic RCC can be difficult because of various factors, including those related to tumor biology, such as tumor heterogeneity, and those related to the type of treatment.

Locally Advanced Disease

RCC can manifest with local infiltration into perirenal fat, adjacent organs, and posterior or lateral abdominal wall musculature. Extension outside the kidney does not necessarily affect the assessment of response in the primary tumor, which is measured on the basis of standard size criteria. Approximately 4%–9% of patients with RCC present with a tumor thrombus extending into the ipsilateral renal vein, with or without extension into the inferior vena cava (83). Of these, almost 70% are clear cell RCCs and 9% are RCCs with sarcomatoid differentiation (83). Surgical resection is the standard of care for patients with venous tumor thrombus. However, assessment of response to systemic therapy in the tumor thrombus may be necessary in nonsurgical patients and those with an unresectable tumor thrombus after surgery. This assessment may not be straightforward, because tumor thrombus appearance may change because of circulation or pulsatility, and variability in the associated bland thrombus may impair the evaluation of treatment-induced changes in the tumor thrombus.

Previous reports (84–89) in which antiangiogenic drugs were used in the neoadjuvant setting for patients with locally advanced disease have shown conflicting results regarding the reduction in the size of the tumor and the inferior vena cava tumor thrombus to facilitate surgical resection. Despite some encouraging results, the response to these neoadjuvant therapies remains heterogeneous, with a substantial number of primary tumors and tumor thrombi exhibiting no reduction in size. Some of these therapies have been implicated in postoperative wound complications (90).

The role of adjuvant and neoadjuvant immunotherapy in RCC is under investigation (91). Our group (92) reported on the use of stereotactic ablative radiation therapy in two patients with RCC and a level 4 thrombus of the inferior vena cava. Imaging studies showed a decrease in the size of the inferior vena cava tumor thrombus and in enhancement after stereotactic ablative radiation therapy; these results correlated with improvement in symptoms. The use of neoadjuvant stereotactic ablative radiation therapy in a level 2 or greater thrombus of the inferior vena cava in patients with RCC is currently under investigation (93).

Tumor Heterogeneity.—RCC is characterized by tumor heterogeneity, a phenomenon in which different clones of cells with specific genomic alterations coexist in the primary tumor and possibly even metastases (94). Clone selection through systemic therapy drives the growth and survival of certain subclones and possibly more aggressive phenotypes. This can result in the phenomenon of oligoprogression: progression of one or a few sites of disease despite overall stable disease or even response. The radiologist must identify the lesions that are enlarging, because focal therapy may be applied and may allow the patient to continue with a particular systemic therapy (95) (Fig 7).

Treatment-related Challenges.—Response assessment traditionally has relied on size-based criteria, with the Response Evaluation Criteria in Solid Tumors (RECIST) 1.1 as the most commonly used method for response assessment (96). RECIST 1.1 is used for clinical trials, although it is not used routinely in clinical practice. The development of molecular-targeted therapies, including tyrosine kinase, mTOR, and immune checkpoint inhibitors, poses challenges for the RECIST criteria. Compared with traditional cytotoxic therapies, molecular-targeted agents may result in changes in the tumor microenvironment such that a response may not be solely reflected in a change in size (Fig 8). In some cases, the size of lesions may increase secondary to internal hemorrhage or necrosis (97).

These challenges have motivated the use of several alternative tumor shrinkage thresholds such as 10% and 20% long-axis-diameter reductions (98,99). Similarly, several alternative criteria have been proposed, such as those by Choi et al (100); revised Choi (101); and morphology, attenuation, size, and structure (MASS) criteria (102), which attempt to overcome the limitations of RECIST 1.1 (103). In addition to assessment for changes in lesion size, these criteria incorporate assessments of attenuation for determination of a response (Table). Nevertheless, attempting to use these alternative criteria in routine clinical practice is challenging owing to their need for contrast-enhanced studies and the difficulty in compar-

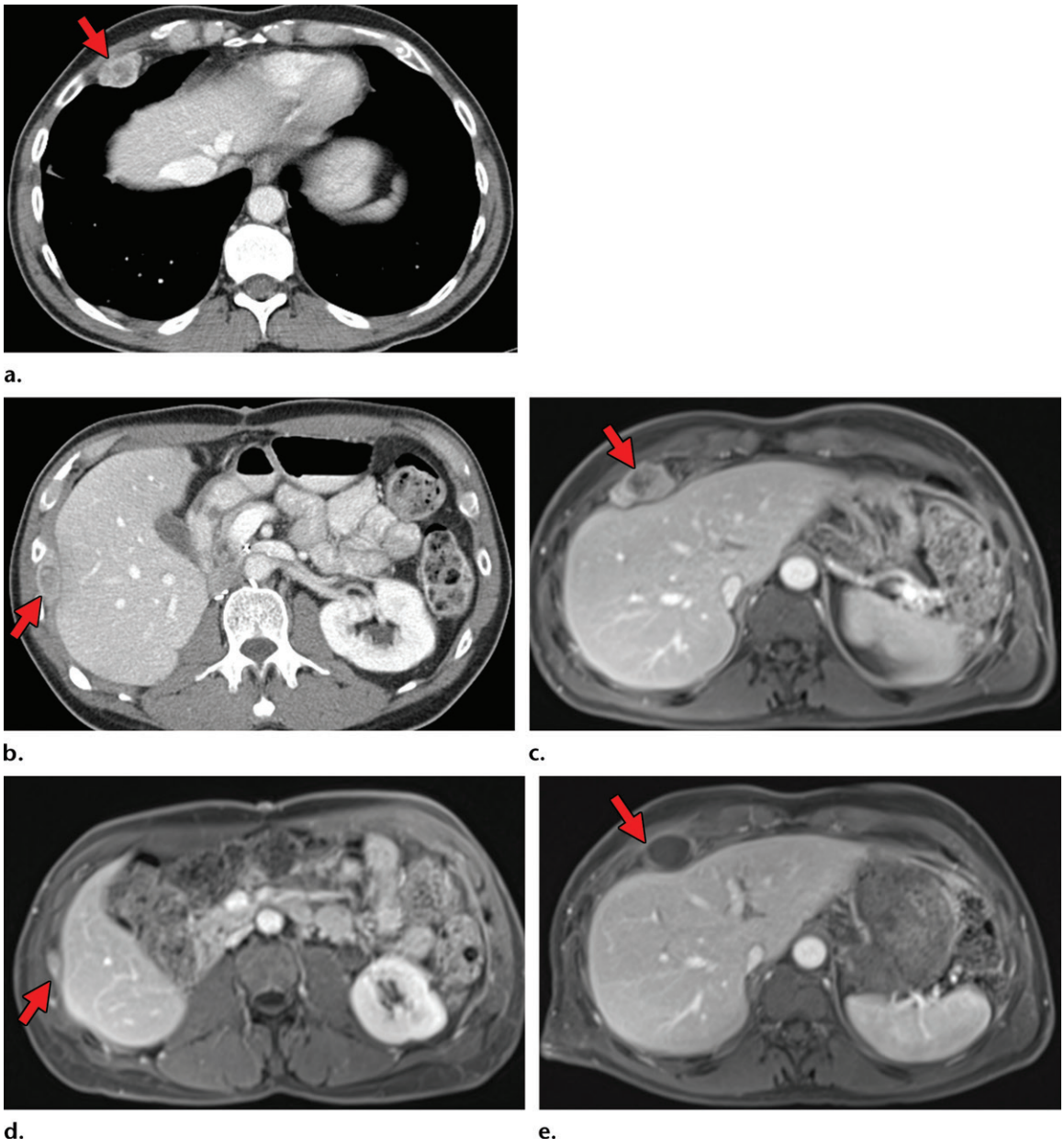

Figure 7. Metastatic clear cell RCC in a 53-year-old man undergoing therapy with nivolumab with oligoprogression. **(a, b)** Axial contrast-enhanced CT images through the lower chest and upper abdomen before the initiation of nivolumab show several extrapleural metastases in the right hemithorax (arrow). The patient subsequently received nivolumab. **(c, d)** Axial contrast-enhanced MR images acquired 6 months after therapy show that most of the lesions decreased in size substantially (arrow in **d**), but one of the metastases had enlarged (arrow in **c**). Another extrapleural metastasis had resolved (not shown). **(e)** Axial contrast-enhanced MR image from an examination after radiation therapy was performed for the enlarging lesion shows a decrease in size and enhancement of the right chest wall lesion (arrow). The patient continued to take nivolumab for an additional 6 months.

ing enhancement at CT and MRI. Others have proposed assessment of response to tyrosine kinase inhibitors with semiautomated solutions that help to measure the vascularized tumor burden (104). These methods may help to decrease interobserver variability in measurements and allow better discrimination between responders and nonresponders to tyrosine kinase inhibitors therapy.

Immune modulators have resulted in a further challenge, because their mechanism of action, through immune and T-cell activation, can result in unusual patterns of response. Infiltration of tumor deposits by immune cells can result in a transient increase in lesion size (and visualization of new lesions) compared with those at initial imaging, followed by tumor regression, which is a phenomenon known as pseudoprogression (Fig 9). This has led to the creation of new immune-related response criteria, such as iRECIST, to assess for response in the setting of immune modulators (105). With iRECIST, for example, the definitions of stable disease, progressive disease, and complete response

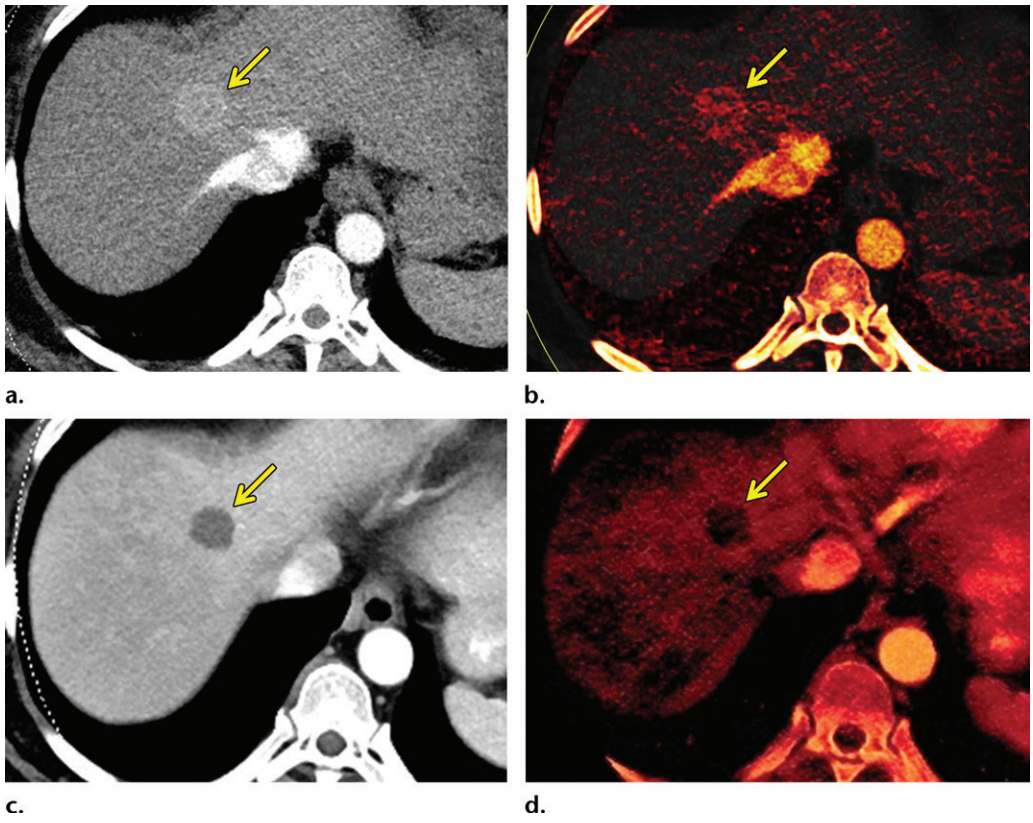

Figure 8. Decrease in enhancement and iodine concentration in a hepatic metastasis of RCC in a 58-year-old woman after treatment with a tyrosine kinase inhibitor. **(a)** Baseline contrast-enhanced CT image of the upper abdomen obtained during the early arterial phase shows an avidly enhancing lesion in the right hepatic lobe (arrow), which is compatible with an RCC metastasis. **(b)** Contrast-enhanced CT image acquired after the initiation of pazopanib shows a decrease in enhancement in the hepatic lesion without a substantial change in size (arrow). **(c, d)** Iodine maps obtained before **(c)** and after **(d)** therapy show a corresponding decrease in iodine concentration (arrow).

Examples of Tumor Response Criteria

Response	RECIST 1.1	iRECIST	Choi	MASS
Progressive disease	≥20% increase in SLD of target lesions compared with nadir; sum must show absolute increase of at least 5 mm; new lesions	Same as RECIST 1.1 but requires that progression be confirmed with imaging assessment within 4–8 weeks	>10% increase in SLD of target lesions; new intratumoral nodule; increase in size of preexisting intratumoral nodule	Unfavorable response: ≥20% increase in SLD in absence of central necrosis or decreased attenuation; new lesions; increase in attenuation of previously nonenhancing mass
Stable disease	Does not fulfill criteria for progressive disease or partial response	Same as RECIST 1.1	Does not fulfill criteria for progressive disease or partial response	Indeterminate response: does not fulfill criteria for unfavorable or favorable response
Partial response	≥30% decrease in SLD of target lesions compared with baseline	Same as RECIST 1.1	>15% decrease in tumor attenuation or >10% decrease in SLD of target lesion	Favorable response: central necrosis or decreased attenuation of one or more solid lesions or decrease in SLD by active surveillance ≥20%
Complete response	Disappearance of all target lesions	Same as RECIST 1.1	Same as RECIST 1.1	…

Sources.—References 94, 98, 100, and 103.
Note.—SLD = sum of the longest diameter.

Figure 9. Pseudoprogression after initiation of nivolumab in a 69-year-old man with metastatic clear cell RCC. **(a)** Baseline axial CT image of the chest shows several right pulmonary metastases (arrows), which had enlarged when compared with prior images (not shown). **(b)** Axial CT image from a follow-up examination 1 month after treatment with nivolumab shows continued enlargement of the pulmonary metastases (arrows). Images of the abdomen at that time also showed new hepatic and pancreatic metastases (not shown). Given these findings and poor performance status, the patient decided to forego further treatment and pursue hospice care. After 6 months, the patient returned to clinical care with substantially improved performance status. **(c)** Axial CT image obtained at that time shows substantial improvement in pulmonary disease. Several of the pulmonary metastases previously visualized in the right middle and lower lobes are no longer seen. The hepatic and pancreatic metastases had decreased substantially in size (not shown). The rapid enlargement on the initial follow-up image in **b** is in keeping with pseudoprogression, which is the result of a transient inflammatory infiltration to the tumor by immune cells and a part of the pathophysiology of response for immune checkpoint inhibitors.

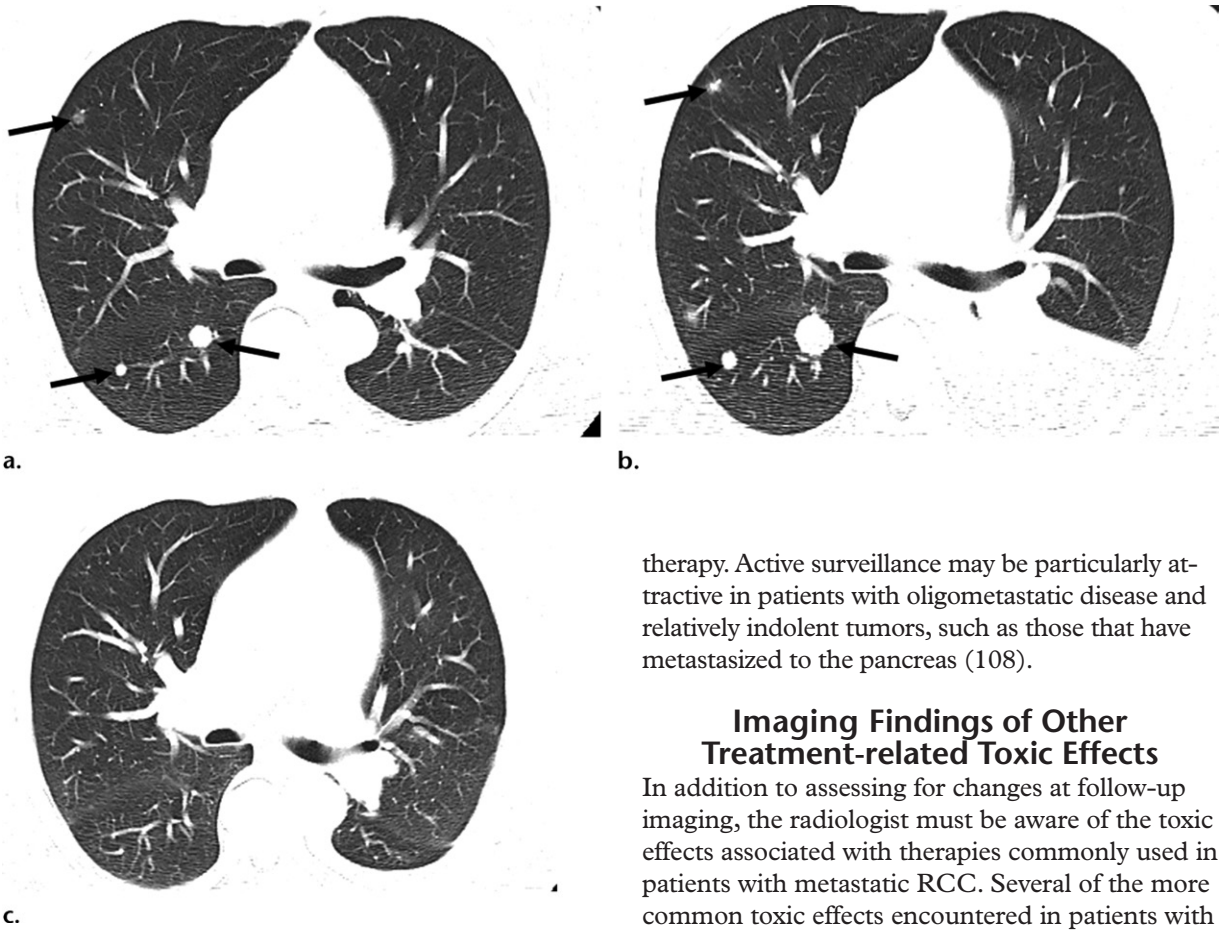

are identical to those of RECIST 1.1. However, if progressive disease is identified at initial imaging after initiation of therapy, progressive disease must be confirmed at follow-up imaging within 4–8 weeks to ensure that pseudoprogression has not occurred.

Active Surveillance.—The role of active surveillance in patients with metastatic RCC is increasing. These patients present with a prolonged, indolent course of disease exhibiting acceptable progression-free survival compared with patients undergoing systemic therapy (106). A phase 2 trial (107) reported shorter surveillance periods for patients with higher numbers of International Metastatic Database Consortium (IMDC) adverse risk factors and of metastatic disease sites. The authors concluded that a subset of patients with metastatic RCC can undergo surveillance safely before starting systemic therapy. Active surveillance may be particularly attractive in patients with oligometastatic disease and relatively indolent tumors, such as those that have metastasized to the pancreas (108).

Imaging Findings of Other Treatment-related Toxic Effects

In addition to assessing for changes at follow-up imaging, the radiologist must be aware of the toxic effects associated with therapies commonly used in patients with metastatic RCC. Several of the more common toxic effects encountered in patients with RCC are described in the sections that follow.

Gastrointestinal Tract Toxic Effects

Gastrointestinal toxic effects may occur with various agents, including mTOR, tyrosine kinase, and immune checkpoint inhibitors. Inflammation of the gastrointestinal tract (eg, enteritis, colitis) is a known immune-related adverse event that is associated with immune checkpoint inhibition therapy and is thought to be secondary to inflammatory cell infiltration in the gastrointestinal mucosa. Prior studies (109–111) reported an incidence of 21% for this adverse event. At endoscopy, immune-mediated enteritis can appear similar to inflammatory bowel disease, and friability, ulcerations, and spontaneous bleeding have been described. Depending on the severity, corticosteroids may be administered. At imaging, immune-mediated colitis more commonly appears as diffuse colonic wall thickening with pericolonic

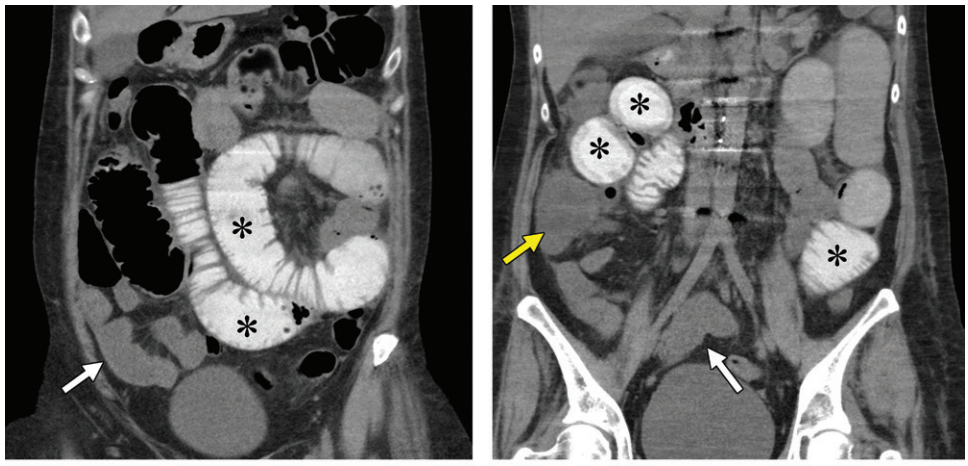

a. b.

Figure 10. Metastatic clear cell RCC with enteritis in a 55-year-old woman who underwent checkpoint inhibition therapy. The patient developed abdominal pain and high-grade diarrhea after completion of a second cycle of combination therapy with ipilimumab and nivolumab. Coronal reconstructions of a non-enhanced CT examination reveal dilatation of proximal small bowel loops filled with oral contrast material (*), with fluid-filled nondistended loops of the distal small bowel (white arrow). Note the fluid-filled cecum (yellow arrow in **b**) in the right lower quadrant. Small-bowel biopsy results confirmed findings consistent with immunomodulatory enteritis.

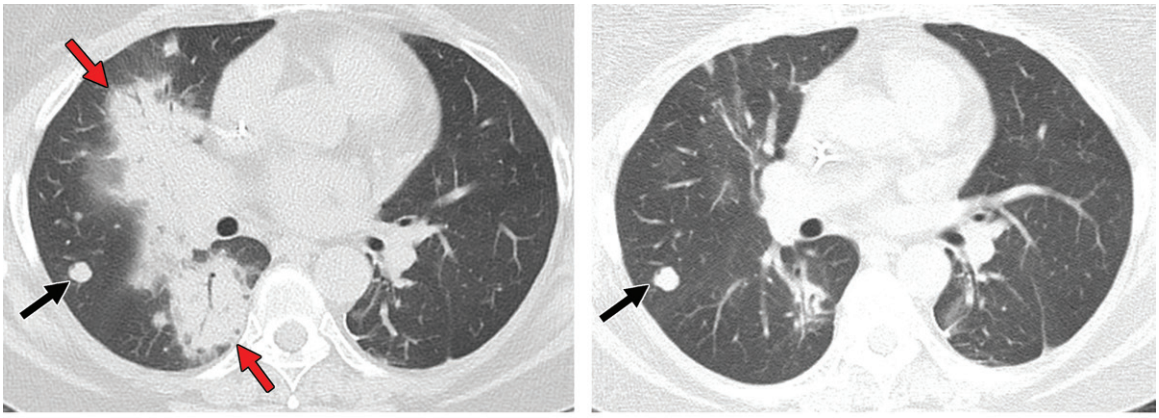

a. b.

Figure 11. Pneumonitis associated with nivolumab therapy in a 61-year-old woman with metastatic clear cell RCC. The patient presented in the emergency department with shortness of breath 1 month after the initiation of nivolumab therapy. **(a)** Axial CT image of the chest shows patchy peribronchovascular consolidation, which is most pronounced in the right lower and middle lobes (red arrows). The nivolumab therapy subsequently was stopped, and the patient was given corticosteroids. Black arrow = right middle lobe metastasis. **(b)** Axial CT image of the chest obtained 1 month later shows near-complete resolution of consolidation. Arrow = right middle lobe metastasis.

fat stranding and mesenteric vessel engorgement, although segmental patterns also have been described (112). In addition, enteritis or colitis may occur in isolation (Fig 10).

Numerous case reports (113–116) have documented pneumatosis intestinalis secondary to tyrosine kinase inhibitors, but the exact incidence is unknown (113). A few mechanisms of tyrosine kinase inhibitor–induced pneumatosis intestinalis have been proposed, including compromised bowel wall integrity and disruption, necrosis of serosal tumor implants, and impaired healing (114). In addition, pneumoperitoneum has been reported to occur with tyrosine kinase inhibitor–induced pneumatosis intestinalis. Patients may be asymptomatic, and a report (115) described conservative treatment of pneumatosis with or without pneumoperitoneum, but life-threatening cases of pneumatosis intestinalis also have been reported (115,116). Nevertheless, to our knowledge, it is not possible to differentiate with imaging the patients who may benefit from conservative treatment from those whose case is life threatening.

Pulmonary Toxic Effects

Pneumonitis occurs in up to 30% of patients who receive treatment with mTOR inhibitors and has been associated with therapeutic benefit

(117). Pneumonitis is also a known uncommon but potentially fatal adverse event associated with immune checkpoint inhibitors. One meta-analysis (118) reported an overall incidence of 2.7% . The time of onset after initiation of therapy is variable, with a median time of nearly 3 months, although it has been reported to occur between 2 and 24 months (119).

At imaging, the most frequently reported pattern is cryptogenic organizing pneumonia, including consolidation, traction bronchiectasis, and ground-glass and reticular opacities (120) (Fig 11). The second most common manifestation is nonspecific interstitial pneumonia, including reticular and ground-glass opacities with a lower lobe predominance. Hypersensitivity pneumonitis and acute interstitial patterns have also been described.

The management of pneumonitis depends on the grade, which is affected by the presence and severity of symptoms. For those with mild to moderate symptoms, checkpoint inhibition therapy is held and steroids are administered; for those with severe symptoms including hypoxia and respiratory compromise, patients most often are admitted to the hospital, and intravenous steroid therapy is administered with or without additional immunosuppression.

Conclusion

Locally advanced and metastatic RCC present a specific set of challenges to the radiologist that may affect the detection of disease, assessment of disease response, and recognition of toxicity-related imaging findings. Nevertheless, it is vital for the radiologist to be aware of these factors to provide an accurate interpretation of imaging and to assist in the treatment of patients with metastatic RCC.

References

1. Amin MB, Amin MB, Tamboli P, et al. Prognostic impact of histologic subtyping of adult renal epithelial neoplasms: an experience of 405 cases. Am J Surg Pathol 2002;26(3): 281–291.
2. Patard JJ, Leray E, Rioux-Leclercq N, et al. Prognostic value of histologic subtypes in renal cell carcinoma: a multicenter experience. J Clin Oncol 2005;23(12):2763–2771.
3. Siegel RL, Miller KD, Jemal A. Cancer statistics, 2016. CA Cancer J Clin 2016;66(1):7–30.
4. Noone AMHN, Krapcho M, Miller D, et al. SEER cancer statistics review, 1975-2015. Bethesda, Md: National Cancer Institute. https://seer.cancer.gov/csr/1975_2015/. Accessed April 20, 2018.
5. Ross H, Martignoni G, Argani P. Renal cell carcinoma with clear cell and papillary features. Arch Pathol Lab Med 2012;136(4):391–399.
6. Leibovich BC, Lohse CM, Crispen PL, et al. Histological subtype is an independent predictor of outcome for patients with renal cell carcinoma. J Urol 2010;183(4):1309–1315.
7. Teloken PE, Thompson RH, Tickoo SK, et al. Prognostic impact of histological subtype on surgically treated localized renal cell carcinoma. J Urol 2009;182(5):2132–2136.
8. Young JR, Margolis D, Sauk S, Pantuck AJ, Sayre J, Raman SS. Clear cell renal cell carcinoma: discrimination from other renal cell carcinoma subtypes and oncocytoma at multiphasic multidetector CT. Radiology 2013;267(2):444–453.
9. Sun MR, Ngo L, Genega EM, et al. Renal cell carcinoma: dynamic contrast-enhanced MR imaging for differentiation of tumor subtypes--correlation with pathologic findings. Radiology 2009;250(3):793–802.
10. Rosenkrantz AB, Niver BE, Fitzgerald EF, Babb JS, Chandarana H, Melamed J. Utility of the apparent diffusion coefficient for distinguishing clear cell renal cell carcinoma of low and high nuclear grade. AJR Am J Roentgenol 2010;195(5):W344–W351.
11. Wang H, Cheng L, Zhang X, et al. Renal cell carcinoma: diffusion-weighted MR imaging for subtype differentiation at 3.0 T. Radiology 2010;257(1):135–143.
12. Delahunt B, Eble JN. Papillary renal cell carcinoma: a clinicopathologic and immunohistochemical study of 105 tumors. Mod Pathol 1997;10(6):537–544.
13. Moch H, Cubilla AL, Humphrey PA, Reuter VE, Ulbright TM. The 2016 WHO classification of tumours of the urinary system and male genital organs—part A: renal, penile, and testicular tumours. Eur Urol 2016;70(1):93–105.
14. Egbert ND, Caoili EM, Cohan RH, et al. Differentiation of papillary renal cell carcinoma subtypes on CT and MRI. AJR Am J Roentgenol 2013;201(2):347–355.
15. Yamada T, Endo M, Tsuboi M, et al. Differentiation of pathologic subtypes of papillary renal cell carcinoma on CT. AJR Am J Roentgenol 2008;191(5):1559–1563.
16. Grubb RL 3rd, Franks ME, Toro J, et al. Hereditary leiomyomatosis and renal cell cancer: a syndrome associated with an aggressive form of inherited renal cancer. J Urol 2007;177(6):2074–2079; discussion 2079–2080.
17. Ricketts CJ, Shuch B, Vocke CD, et al. Succinate dehydrogenase kidney cancer: an aggressive example of the Warburg effect in cancer. J Urol 2012;188(6):2063–2071.
18. Amin MB, MacLennan GT, Gupta R, et al. Tubulocystic carcinoma of the kidney: clinicopathologic analysis of 31 cases of a distinctive rare subtype of renal cell carcinoma. Am J Surg Pathol 2009;33(3):384–392.
19. Banerjee I, Yadav SS, Tomar V, Yadav S, Talreja S. Tubulocystic renal cell carcinoma: a great imitator. Rev Urol 2016;18(2):118–121.
20. Cornelis F, Hélénon O, Correas JM, et al. Tubulocystic renal cell carcinoma: a new radiological entity. Eur Radiol 2016;26(4):1108–1115.
21. Choyke PL. Acquired cystic kidney disease. Eur Radiol 2000;10(11):1716–1721.
22. Tickoo SK, dePeralta-Venturina MN, Harik LR, et al. Spectrum of epithelial neoplasms in end-stage renal disease: an experience from 66 tumor-bearing kidneys with emphasis on histologic patterns distinct from those in sporadic adult renal neoplasia. Am J Surg Pathol 2006;30(2):141–153.
23. Ahn S, Kwon GY, Cho YM, et al. Acquired cystic disease-associated renal cell carcinoma: further characterization of the morphologic and immunopathologic features. Med Mol Morphol 2013;46(4):225–232.
24. Gobbo S, Eble JN, Grignon DJ, et al. Clear cell papillary renal cell carcinoma: a distinct histopathologic and molecular genetic entity. Am J Surg Pathol 2008;32(8):1239–1245.
25. Adam J, Couturier J, Molinié V, Vieillefond A, Sibony M. Clear-cell papillary renal cell carcinoma: 24 cases of a distinct low-grade renal tumour and a comparative genomic hybridization array study of seven cases. Histopathology 2011;58(7):1064–1071.
26. Aydin H, Chen L, Cheng L, et al. Clear cell tubulopapillary renal cell carcinoma: a study of 36 distinctive low-grade epithelial tumors of the kidney. Am J Surg Pathol 2010;34(11):1608–1621.
27. Wang K, Zarzour J, Rais-Bahrami S, Gordetsky J. Clear cell papillary renal cell carcinoma: new clinical and imaging characteristics. Urology 2017;103:136–141.
28. Mnatzakanian GN, Shinagare AB, Sahni VA, Hirsch MS, Silverman SG. Early-stage clear cell tubulopapillary renal cell carcinoma: imaging features and distinction from clear cell and papillary subtypes. Abdom Radiol (NY) 2016;41(11):2187–2195.

29. Kaelin WG Jr. The von Hippel-Lindau tumor suppressor protein and clear cell renal carcinoma. Clin Cancer Res 2007;13(2 Pt 2):680s–684s.
30. Hudson CC, Liu M, Chiang GG, et al. Regulation of hypoxia-inducible factor 1alpha expression and function by the mammalian target of rapamycin. Mol Cell Biol 2002;22(20):7004–7014.
31. Wallace EM, Rizzi JP, Han G, et al. A small-molecule antagonist of HIF2a is efficacious in preclinical models of renal cell carcinoma. Cancer Res 2016;76(18):5491–5500.
32. Courtney KD, Infante JR, Lam ET, et al. Phase I dose-escalation trial of PT2385: a first-in-class hypoxia-inducible factor-2α antagonist in patients with previously treated advanced clear cell renal cell carcinoma. J Clin Oncol 2018; 36(9):867-874.
33. Chen W, Hill H, Christie A, et al. Targeting renal cell carcinoma with a HIF-2 antagonist. Nature 2016; 539(7627):112-117.
34. Kanamaru H, Sasaki M, Miwa Y, Akino H, Okada K. Prognostic value of sarcomatoid histology and volume-weighted mean nuclear volume in renal cell carcinoma. BJU Int 1999;83(3):222–226.
35. Frank I, Blute ML, Cheville JC, et al. A multifactorial postoperative surveillance model for patients with surgically treated clear cell renal cell carcinoma. J Urol 2003;170(6 Pt 1):2225–2232.
36. Lam JS, Shvarts O, Leppert JT, Figlin RA, Belldegrun AS. Renal cell carcinoma 2005: new frontiers in staging, prognostication and targeted molecular therapy. J Urol 2005;173(6):1853–1862.
37. Joshi SS, Handorf EA, Zibelman M, et al. Treatment facility volume and survival in patients with metastatic renal cell carcinoma: a registry-based analysis. Eur Urol 2018;74(3):387–393.
38. Janzen NK, Kim HL, Figlin RA, Belldegrun AS. Surveillance after radical or partial nephrectomy for localized renal cell carcinoma and management of recurrent disease. Urol Clin North Am 2003;30(4):843–852.
39. Donat SM, Diaz M, Bishoff JT, et al. Follow-up for clinically localized renal neoplasms: AUA guideline. J Urol 2013;190(2):407–416.
40. Klatte T, Lam JS, Shuch B, Belldegrun AS, Pantuck AJ. Surveillance for renal cell carcinoma: why and how? When and how often? Urol Oncol 2008;26(5):550–554.
41. Stephenson AJ, Chetner MP, Rourke K, et al. Guidelines for the surveillance of localized renal cell carcinoma based on the patterns of relapse after nephrectomy. J Urol 2004;172(1):58–62.
42. Hafez KS, Novick AC, Campbell SC. Patterns of tumor recurrence and guidelines for followup after nephron sparing surgery for sporadic renal cell carcinoma. J Urol 1997;157(6):2067–2070.
43. Bianchi M, Sun M, Jeldres C, et al. Distribution of metastatic sites in renal cell carcinoma: a population-based analysis. Ann Oncol 2012;23(4):973–980.
44. Davenport MS, Khalatbari S, Cohan RH, Dillman JR, Myles JD, Ellis JH. Contrast material-induced nephrotoxicity and intravenous low-osmolality iodinated contrast material: risk stratification by using estimated glomerular filtration rate. Radiology 2013;268(3):719–728.
45. Scatarige JC, Horton KM, Sheth S, Fishman EK. Pancreatic parenchymal metastases: observations on helical CT. AJR Am J Roentgenol 2001;176(3):695–699.
46. Jain Y, Liew S, Taylor MB, Bonington SC. Is dual-phase abdominal CT necessary for the optimal detection of metastases from renal cell carcinoma? Clin Radiol 2011;66(11):1055–1059.
47. Jee HB, Park MJ, Lee HS, Park MS, Kim MJ, Chung YE. Is non-contrast CT adequate for the evaluation of hepatic metastasis in patients who cannot receive iodinated contrast media? PLoS One 2015;10(7):e0134133.
48. ACR Manual on Contrast Media Version 10.3. ACR Committee on Drugs and Contrast Media. https://www.acr.org/Clinical-Resources/Contrast-Manual. Updated 2017. Accessed April 23, 2019.
49. Heffess CS, Wenig BM, Thompson LD. Metastatic renal cell carcinoma to the thyroid gland: a clinicopathologic study of 36 cases. Cancer 2002;95(9):1869–1878.
50. Selvi F, Faquin WC, Michaelson MD, August M. Three synchronous atypical metastases of clear cell renal carcinoma to the maxillary gingiva, scalp and the distal phalanx of the fifth digit: a case report. J Oral Maxillofac Surg 2016;74(6):1286.e1–1286.e9.
51. Gitto S, Vaiani M, Cascella T, Lanocita R. Penile metastases from renal cell carcinoma: pre and postcontrast sonographic findings. Ultrasound Q 2018 Mar 5 [Epub ahead of print].
52. Dionigi G, Uccella S, Gandolfo M, et al. Solitary intrathyroidal metastasis of renal clear cell carcinoma in a toxic substernal multinodular goiter. Thyroid Res 2008;1(1):6.
53. Brufau BP, Cerqueda CS, Villalba LB, Izquierdo RS, González BM, Molina CN. Metastatic renal cell carcinoma: radiologic findings and assessment of response to targeted antiangiogenic therapy by using multidetector CT. RadioGraphics 2013;33(6):1691–1716.
54. Park HJ, Kim HJ, Park SH, Lee JS, Kim AY, Ha HK. Gastrointestinal involvement of recurrent renal cell carcinoma: CT findings and clinicopathologic features. Korean J Radiol 2017;18(3):452–460.
55. Ismail I, Neuen BL, Mantha M. Solitary jejunal metastasis from renal cell carcinoma presenting as small bowel obstruction 19 years after nephrectomy. BMJ Case Rep 2015;2015:bcr2015210857.
56. Bellio G, Cipolat Mis T, Kaso G, Dattola R, Casagranda B, Bortul M. Small bowel intussusception from renal cell carcinoma metastasis: a case report and review of the literature. J Med Case Rep 2016;10(1):222.
57. Tartar VM, Heiken JP, McClennan BL. Renal cell carcinoma presenting with diffuse peritoneal metastases: CT findings. J Comput Assist Tomogr 1991;15(3):450–453.
58. Johnsen JA, Hellsten S. Lymphatogenous spread of renal cell carcinoma: an autopsy study. J Urol 1997;157(2):450–453.
59. Eggener SE, Yossepowitch O, Pettus JA, Snyder ME, Motzer RJ, Russo P. Renal cell carcinoma recurrence after nephrectomy for localized disease: predicting survival from time of recurrence. J Clin Oncol 2006;24(19):3101–3106.
60. Abara E, Chivulescu I, Clerk N, Cano P, Goth A. Recurrent renal cell cancer: 10 years or more after nephrectomy. Can Urol Assoc J 2010;4(2):E45–E49.
61. Riviello C, Tanini I, Cipriani G, et al. Unusual gastric and pancreatic metastatic renal cell carcinoma presentation 10 years after surgery and immunotherapy: a case report and a review of literature. World J Gastroenterol 2006;12(32):5234–5236.
62. Wolf S, Obolonczyk L, Sworczak K, Czapiewski P, Sledzinski Z. Renal cell carcinoma metastases to the pancreas and the thyroid gland 19 years after the primary tumour. Prz Gastroenterol 2015;10(3):185–189.
63. Faure JP, Tuech JJ, Richer JP, Pessaux P, Arnaud JP, Carretier M. Pancreatic metastasis of renal cell carcinoma: presentation, treatment and survival. J Urol 2001;165(1):20–22.
64. Kalra S, Atkinson BJ, Matrana MR, et al. Prognosis of patients with metastatic renal cell carcinoma and pancreatic metastases. BJU Int 2016;117(5):761–765.
65. Zerbi A, Ortolano E, Balzano G, Borri A, Beneduce AA, Di Carlo V. Pancreatic metastasis from renal cell carcinoma: which patients benefit from surgical resection? Ann Surg Oncol 2008;15(4):1161–1168.
66. Mechó S, Quiroga S, Cuéllar H, Sebastià C. Pancreatic metastasis of renal cell carcinoma: multidetector CT findings. Abdom Imaging 2009;34(3):385–389.
67. Sikka A, Adam SZ, Wood C, Hoff F, Harmath CB, Miller FH. Magnetic resonance imaging of pancreatic metastases from renal cell carcinoma. Clin Imaging 2015;39(6):945–953.
68. Ballarin R, Spaggiari M, Cautero N, et al. Pancreatic metastases from renal cell carcinoma: the state of the art. World J Gastroenterol 2011;17(43):4747–4756.
69. Miller FH, Rini NJ, Keppke AL. MRI of adenocarcinoma of the pancreas. AJR Am J Roentgenol 2006;187(4): W365–W374.
70. Tamm EP, Silverman PM, Charnsangavej C, Evans DB. Diagnosis, staging, and surveillance of pancreatic cancer. AJR Am J Roentgenol 2003;180(5):1311–1323.
71. Kang TW, Kim SH, Lee J, et al. Differentiation between pancreatic metastases from renal cell carcinoma and hypervascular neuroendocrine tumour: use of relative percentage

washout value and its clinical implication. Eur J Radiol 2015;84(11):2089–2096.
72. Choi YA, Kim CK, Park BK, Kim B. Evaluation of adrenal metastases from renal cell carcinoma and hepatocellular carcinoma: use of delayed contrast-enhanced CT. Radiology. 2013;266(2):514-20.
73. Schieda N, Krishna S, McInnes MDF, Moosavi B, Alrashed A, Moreland R, et al. Utility of MRI to Differentiate Clear Cell Renal Cell Carcinoma Adrenal Metastases From Adrenal Adenomas. AJR Am J Roentgenol. 2017;209(3):W152-w9.
74. Santini D, Procopio G, Porta C, et al. Natural history of malignant bone disease in renal cancer: final results of an Italian bone metastasis survey. PLoS One 2013;8(12):e83026.
75. Schweitzer ME, Levine C, Mitchell DG, Gannon FH, Gomella LG. Bull's-eyes and halos: useful MR discriminators of osseous metastases. Radiology 1993;188(1):249–252.
76. Staudenherz A, Steiner B, Puig S, Kainberger F, Leitha T. Is there a diagnostic role for bone scanning of patients with a high pretest probability for metastatic renal cell carcinoma? Cancer 1999;85(1):153–155.
77. Gerety EL, Lawrence EM, Wason J, et al. Prospective study evaluating the relative sensitivity of 18F-NaF PET/CT for detecting skeletal metastases from renal cell carcinoma in comparison to multidetector CT and 99mTc-MDP bone scintigraphy, using an adaptive trial design. Ann Oncol 2015;26(10):2113–2118.
78. Schmidt GP, Baur-Melnyk A, Haug A, et al. Comprehensive imaging of tumor recurrence in breast cancer patients using whole-body MRI at 1.5 and 3 T compared to FDG-PET-CT. Eur J Radiol 2008;65(1):47–58.
79. Schmidt GP, Baur-Melnyk A, Haug A, et al. Whole-body MRI at 1.5 T and 3 T compared with FDG-PET-CT for the detection of tumour recurrence in patients with colorectal cancer. Eur Radiol 2009;19(6):1366–1378.
80. Ng SH, Chan SC, Yen TC, et al. Comprehensive imaging of residual/ recurrent nasopharyngeal carcinoma using whole-body MRI at 3 T compared with FDG-PET-CT. Eur Radiol 2010;20(9):2229–2240.
81. Platzek I, Zastrow S, Deppe PE, et al. Whole-body MRI in follow-up of patients with renal cell carcinoma. Acta Radiol 2010;51(5):581–589.
82. Sohaib SA, Cook G, Allen SD, Hughes M, Eisen T, Gore M. Comparison of whole-body MRI and bone scintigraphy in the detection of bone metastases in renal cancer. Br J Radiol 2009;82(980):632–639.
83. Zisman A, Wieder JA, Pantuck AJ, et al. Renal cell carcinoma with tumor thrombus extension: biology, role of nephrectomy and response to immunotherapy. J Urol 2003;169(3):909–916.
84. Zhang Y, Li Y, Deng J, Ji Z, Yu H, Li H. Sorafenib neoadjuvant therapy in the treatment of high risk renal cell carcinoma. PLoS One 2015;10(2):e0115896.
85. Hellenthal NJ, Underwood W, Penetrante R, et al. Prospective clinical trial of preoperative sunitinib in patients with renal cell carcinoma. J Urol 2010;184(3):859–864.
86. van der Veldt AA, Meijerink MR, van den Eertwegh AJ, et al. Sunitinib for treatment of advanced renal cell cancer: primary tumor response. Clin Cancer Res 2008;14(8):2431–2436.
87. Jonasch E, Wood CG, Matin SF, et al. Phase II presurgical feasibility study of bevacizumab in untreated patients with metastatic renal cell carcinoma. J Clin Oncol 2009;27(25):4076–4081.
88. Rini BI, Garcia J, Elson P, et al. The effect of sunitinib on primary renal cell carcinoma and facilitation of subsequent surgery. J Urol 2012;187(5):1548–1554.
89. Cost NG, Delacroix SE Jr, Sleeper JP, et al. The impact of targeted molecular therapies on the level of renal cell carcinoma vena caval tumor thrombus. Eur Urol 2011;59(6):912–918.
90. Borregales LD, Adibi M, Thomas AZ, Wood CG, Karam JA. The role of neoadjuvant therapy in the management of locally advanced renal cell carcinoma. Ther Adv Urol 2016;8(2):130–141.
91. Choueiri M, Tannir N, Jonasch E. Adjuvant and neoadjuvant therapy in renal cell carcinoma. Curr Clin Pharmacol 2011;6(3):144–150.
92. Hannan R, Margulis V, Chun SG, et al. Stereotactic radiation therapy of renal cancer inferior vena cava tumor thrombus. Cancer Biol Ther 2015;16(5):657–661.
93. Freifeld Y, Hannan R, Woldu S, et al. LBA28 safety lead-in of a phase II trial of neo-adjuvant SABR for IVC tumor thrombus in RCC. J Urol 2018;199(4):e1168.
94. Gerlinger M, Rowan AJ, Horswell S, et al. Intratumor heterogeneity and branched evolution revealed by multiregion sequencing. N Engl J Med 2012;366(10):883–892.
95. Straka C, Kim DW, Timmerman RD, Pedrosa I, Jacobs C, Brugarolas J. Ablation of a site of progression with stereotactic body radiation therapy extends sunitinib treatment from 14 to 22 months. J Clin Oncol 2013;31(23):e401–e403.
96. Eisenhauer EA, Therasse P, Bogaerts J, et al. New response evaluation criteria in solid tumours: revised RECIST guideline (version 1.1). Eur J Cancer 2009;45(2):228–247.
97. Choi H, Charnsangavej C, de Castro Faria S, et al. CT evaluation of the response of gastrointestinal stromal tumors after imatinib mesylate treatment: a quantitative analysis correlated with FDG PET findings. AJR Am J Roentgenol 2004;183(6):1619–1628.
98. Thiam R, Fournier LS, Trinquart L, et al. Optimizing the size variation threshold for the CT evaluation of response in metastatic renal cell carcinoma treated with sunitinib. Ann Oncol 2010;21(5):936–941.
99. Krajewski KM, Guo M, Van den Abbeele AD, et al. Comparison of four early posttherapy imaging changes (EPTIC; RECIST 1.0, tumor shrinkage, computed tomography tumor density, Choi criteria) in assessing outcome to vascular endothelial growth factor-targeted therapy in patients with advanced renal cell carcinoma. Eur Urol 2011;59(5):856–862.
100. Choi H, Charnsangavej C, Faria SC, et al. Correlation of computed tomography and positron emission tomography in patients with metastatic gastrointestinal stromal tumor treated at a single institution with imatinib mesylate: proposal of new computed tomography response criteria. J Clin Oncol 2007;25(13):1753–1759.
101. Thian Y, Gutzeit A, Koh DM, et al. Revised Choi imaging criteria correlate with clinical outcomes in patients with metastatic renal cell carcinoma treated with sunitinib. Radiology 2014;273(2):452–461.
102. Smith AD, Shah SN, Rini BI, Lieber ML, Remer EM. Morphology, attenuation, size, and structure (MASS) criteria: assessing response and predicting clinical outcome in metastatic renal cell carcinoma on antiangiogenic targeted therapy. AJR Am J Roentgenol 2010;194(6):1470–1478.
103. Tirkes T, Hollar MA, Tann M, Kohli MD, Akisik F, Sandrasegaran K. Response criteria in oncologic imaging: review of traditional and new criteria. RadioGraphics 2013;33(5):1323–1341.
104. Smith AD, Zhang X, Bryan J, et al. Vascular tumor burden as a new quantitative CT biomarker for predicting metastatic RCC response to antiangiogenic therapy. Radiology 2016;281(2):484–498.
105. Seymour L, Bogaerts J, Perrone A, et al. iRECIST: guidelines for response criteria for use in trials testing immunotherapeutics. Lancet Oncol 2017;18(3):e143–e152.
106. Matsubara N, Mukai H, Naito Y, Itoh K, Komai Y, Sakai Y. First experience of active surveillance before systemic target therapy in patients with metastatic renal cell carcinoma. Urology 2013;82(1):118–123.
107. Rini BI, Dorff TB, Elson P, et al. Active surveillance in metastatic renal-cell carcinoma: a prospective, phase 2 trial. Lancet Oncol 2016;17(9):1317–1324.
108. Sbitti Y, Seddik H, Debbagh A, et al. Metachronous pancreatic metastases from renal cell carcinoma: is there a place of active-surveillance before deferred deliberately molecular target agent? World J Surg Oncol 2016;14(1):222.
109. Beck KE, Blansfield JA, Tran KQ, et al. Enterocolitis in patients with cancer after antibody blockade of cytotoxic T-lymphocyte-associated antigen 4. J Clin Oncol 2006;24(15):2283–2289.
110. Berman D, Parker SM, Siegel J, et al. Blockade of cytotoxic T-lymphocyte antigen-4 by ipilimumab results in dysregulation of gastrointestinal immunity in patients with advanced melanoma. Cancer Immun 2010;10:11.
111. Yang JC, Hughes M, Kammula U, et al. Ipilimumab (anti-CTLA4 antibody) causes regression of metastatic renal cell cancer associated with enteritis and hypophysitis. J Immunother 2007;30(8):825-30.

112. Kim KW, Ramaiya NH, Krajewski KM, et al. Ipilimumab-associated colitis: CT findings. AJR Am J Roentgenol 2013;200(5):W468–W474.
113. Kameda T, Nakano K, Yamazaki M, Koshimizu T, Morita T. Axitinib-induced pneumatosis intestinalis and acute acalculous cholecystitis in a patient with renal cell carcinoma. Urology 2017;101:e7–e8.
114. Coriat R, Ropert S, Mir O, et al. Pneumatosis intestinalis associated with treatment of cancer patients with the vascular growth factor receptor tyrosine kinase inhibitors sorafenib and sunitinib. Invest New Drugs 2011;29(5):1090–1093.
115. Shinagare AB, Howard SA, Krajewski KM, Zukotynski KA, Jagannathan JP, Ramaiya NH. Pneumatosis intestinalis and bowel perforation associated with molecular targeted therapy: an emerging problem and the role of radiologists in its management. AJR Am J Roentgenol 2012;199(6):1259–1265.
116. Kashima T, Ohno Y, Tachibana M. Pneumatosis intestinalis and hepatic portal venous gas in a patient receiving sorafenib. Int J Urol 2012;19(11):1041–1042.
117. Dabydeen DA, Jagannathan JP, Ramaiya N, et al. Pneumonitis associated with mTOR inhibitors therapy in patients with metastatic renal cell carcinoma: incidence, radiographic findings and correlation with clinical outcome. Eur J Cancer 2012;48(10):1519–1524.
118. Nishino M, Giobbie-Hurder A, Hatabu H, Ramaiya NH, Hodi FS. Incidence of programmed cell death 1 inhibitor-related pneumonitis in patients with advanced cancer: a systematic review and meta-analysis. JAMA Oncol 2016;2(12):1607–1616.
119. Naidoo J, Wang X, Woo KM, et al. Pneumonitis in patients treated with anti-programmed death-1/programmed death ligand 1 therapy. J Clin Oncol 2017;35(7):709–717.
120. Nishino M, Ramaiya NH, Awad MM, et al. PD-1 inhibitor-related pneumonitis in advanced cancer patients: radiographic patterns and clinical course. Clin Cancer Res 2016;22(24):6051–6060.